Physiological and comparative proteomic analyzes reveal immune defense response of the king scallop Pecten maximus in presence of paralytic shellfish toxin (PST) from Alexandrium minutum

Yasmine Even, Emilien Pousse, Coraline Chapperon, Sébastien Artigaud, Hélène Hégaret, Benoit Bernay, Vianney Pichereau, Jonathan Flye-Sainte-Marie, Fred Jean

Physiological and comparative proteomic analyzes reveal immune defense response of the king scallop *Pecten maximus* in presence of paralytic shellfish toxin (PST) from *Alexandrium minutum.*

Authors: Yasmine Even[1*], Emilien Pousse[1], Coraline Chapperon[1], Sébastien Artigaud[1], Hélène Hégaret[1], Benoit Bernay[2], Vianney Pichereau[1], Jonathan Flye-Sainte-Marie[1], Fred Jean[1].

1: Laboratoire des Sciences de l'Environnement Marin, UMR 6539 CNRS/UBO – Institut Universitaire Européen de la Mer, Technopôle Brest-Iroise, 29280 Plouzané, France

2 : Plateforme Proteogen, US EMerode, Université de Caen Normandie, Esplanade de la paix, 14032 Caen, France

* *Corresponding author:* Dr Yasmine Even, PhD, LEMAR – IUEM, Technopôle Brest-Iroise, 29280 Plouzané, France; yasmine.even@univ-brest.fr; Tel: 33+298 498 670; Fax: 33+298 498 645

Abstract

The king scallop, *Pecten maximus* is a highly valuable seafood in Europe. Over the last few years, its culture has been threatened by toxic microalgae during harmful algal blooms, inducing public health concerns. Indeed, phycotoxins accumulated in bivalves can be harmful for human, especially paralytic shellfish toxins (PST) synthesized by the microalgae *Alexandrium minutum*. Deleterious effects of these toxic algae on bivalves have also been reported. However, its impact on bivalves such as king scallop is far from being completely understood. This study combined ecophysiological and proteomic analyzes to investigate the early response of juvenile king scallops to a short term exposure to PST producing *A. minutum*. Our data showed that all along the 2-days exposure to *A. minutum*, king scallops exhibited transient lower filtration and respiration rates and accumulated PST. Significant inter-individual variability of toxin accumulation potential was observed among individuals. Furthermore, we found that ingestion of toxic algae, correlated to toxin accumulation was driven by two factors: 1/ the time it takes king scallop to recover from filtration inhibition and starts to filtrate again, 2/ the filtration level to which king scallop starts again to filtrate after inhibition. Furthermore, at the end of the 2-day exposure to *A. minutum*, proteomic analyzes revealed an increase of the killer cell lectin-like receptor B1, involved in adaptative immune response. Proteins involved in detoxification and in metabolism were found in lower amount in *A. minutum* exposed king scallops. Proteomic data also showed differential accumulation in several structure proteins such as β-actin, paramyosin and filamin A, suggesting a remodeling of the mantle tissue when king scallops are subjected to an *A. minutum* exposure.

Key words: Paralytic shellfish toxins, *Alexandrium minutum, Pecten maximus,* ecotoxicology, proteomics.

1. Introduction

King scallop, *Pecten maximus* is a highly valued seafood product and is of major commercial importance in Europe with global capture production of 60,000 tons in 2019 (FAO Fisheries and Aquaculture Department). This marine bivalve lives in coastal waters at the surface of, or slightly buried in the sediment (Baird, 1958). Like many shellfishes feeding on microalgae, king scallops are exposed to harmful algal blooms (HAB) (Chauvaud et al., 2001, 1998). HAB occur worldwide and can negatively affect king scallops including hatchery seeds and juveniles (Anderson et al., 2012; Borcier et al., 2017; Li et al., 2002), thus causing significant economic and social impacts. A better understanding of the different effects caused by harmful algae exposures on the king scallop is therefore essential to improve the management of fisheries or aquaculture practices.

Toxic microalgae of the genus *Alexandrium*, are responsible for a large proportion of HAB events worldwide. Indeed, the dinoflagellates *Alexandrium* spp. can produce saxitoxin and its derivatives that are paralytic shellfish toxins (PST), responsible for the paralytic shellfish poisoning (PSP) syndrome in human following consumption of contaminated seafood. The PST can be lethal for mammals by inducing paralysis via binding to voltage-dependent sodium channels involved in the nervous influx, thus inhibiting membrane depolarization and blocking proliferation of action potentials (Narahashi and Moore, 1968; Ritchie and Rogart, 1977). Although less toxic for invertebrates such as bivalves, the consumption of toxic algae such as *Alexandrium minutum* that synthesizes PST, which accumulate within the digestive gland and soft tissues, can results in several deleterious effects (Borcier et al., 2017; Castrec et al., 2018; Contreras et al., 2012a, 2012b; Fabioux et al., 2015; Li et al., 2002; Pousse et al., 2018). Assessing the effect of toxic dinoflagellates upon bivalves is of great importance, as it first represents a hazard for human after consumption of contaminated seafood, but also for other marine organisms exposed to these toxic dinoflagellates, therefore impacting socioeconomic activity, especially associated with the closure of fishing areas, when toxin concentration exceeds authorized values (Anderson et al., 2012; Geraci et al., 1989; Hégaret et al., 2009; Reyero et al., 1999). Among the *A. minutum* species, several strains have been

identified with variable amounts of PST produced, as well as variable levels of cytotoxic potency, associated to the production of some uncharacterized bioactive extracellular components (BEC), independent from PST (Borcier et al., 2017; Castrec et al., 2018; Long et al., 2018). In the latter studies, clear damages of BEC on bivalves or other marine organisms have been demonstrated, whereas toxic effects of PST on bivalves are less well established (Mat et al., 2013; Payton et al., 2017).

The effects of *A. minutum* and its toxins on mussels and oysters have been well studied (Bougrier et al., 2003; Castrec et al., 2019; Fabioux et al., 2015; Haberkorn et al., 2010b, 2010a; Mat et al., 2018; Payton et al., 2017), however very little is known about its physiological impact on the king scallop. Coquereau et al (2016) and Borcier et al (2017) respectively demonstrated that an exposure to *A. minutum,* depending on the strain, could lead to modified valve movement, but also a decreasing filtration rate and shell growth as well as histological damages and altered escape response. No studies have, however, investigated the ecophysiological and associated proteomic responses of the king scallop following an exposure to this toxic microalgae. In order to better understand protective mechanisms activated in bivalves when exposed to toxic algae, we assessed the response of king scallop juveniles to an environmental stress, corresponding to a short term exposure to a PST producing strain of *A. minutum*, by characterizing physiological and proteome modifications in king scallops. More specifically, we measured toxin accumulation in king scallops and its consequences on physiological parameters such as filtration and respiration. We further performed proteomic analyzes on mantle tissues to evaluate the responses of juvenile king scallops to *A. minutum* exposure at the protein levels.

2. Material and methods

2.1. Animals and sample collection

King scallop (*P. maximus)* juveniles were obtained from the Tinduff hatchery (Plougastel-Daoulas, France). Average individual length was 35.9 ± 2.1 mm ($mean \pm SD, n = 35$). In order to make sure that toxin accumulation in king scallops is not due to contaminations prior to our experiment, individuals were acclimated a week prior experiments into seawater (35 PSU) flow-through tanks and fed *ad libitum* with a standard 50/50 mix of algae *Tisochrisis lutea* (T-iso) and *Chaetoceros muelleri* which are common aquaculture feed.

2.2. Algal cultures

T. lutea (strain CCAP 927/14) and *C. muelleri* (strain CCAP1010/3) were produced in continuous (10 L bioreactor) and batch cultures (2 L and 6 L glass bottles) in Conway medium (Walne, 1966) made with UV sterilized 1-µm filtered seawater (35 PSU) that was aerated with a mix of air and CO_2 (Walne, 1970).

Cultures of *A. minutum* (strain Daoulas 1257) were grown in 2 L and 6 L glass bottles with L1 medium (Guillard and Hargraves, 1993) made with 1-µm filtered seawater (35 PSU). Air but no CO_2 was added to the cultures. Room temperature was maintained at 18ºC with a 12:12 photoperiod. The mean toxicity of *A. minutum* strain Daoulas 1257 was 52.8 fg STX equivalent cell^{-1} (equivalent to 0.63 fmol cell−1; Pousse et al., 2018) at the end of the exponential growth phase. This strain was reported to not produce any bioactive extracellular compounds responsible for toxic effects in bivalves (Castrec et al., 2018) or allelopathic effects (Long et al., 2018).

2.3. Exposure to A. minutum and sampling

In order to examine the potential physiological effects of *A. minutum* strain Daoulas 1257 and its PST upon king scallops, experimental trials were divided into 2 phases. Each phase lasted 2 days.

During the first phase, each group of king scallops (n=25) were fed with a normal diet characterized by an equal algal mix of non-toxic algae (50/50, *T. lutea* and *C. muelleri*, for algal concentrations see Fig. 1).

During the second phase, king scallop individuals were exposed to 2 different conditions:

1) absence of food: no algae (NA); experiment named TC-NA hereafter (n=7).

2) toxic diet: *A. minutum* strain Daoulas 1257 (A); experiment repeated 3 times and named TC-A1, TC-A2, TC-A3 (n=18); the concentration of *A. minutum* distributed to king scallops was respectively 560, 440 and 500 cells mL^{-1} (Fig. 1).

During the 4 days, the flow rate in each chamber was adjusted to 30 mL min^{-1}. At the end of the 4 days of experiment, juvenile king scallops were individually measured and weighted (total, shell and humid flesh mass) and mantles were collected and stored at -80°C for further proteomic analyzes. For specimen exposed to *A. minutum* the digestive gland was collected, weighted and stored at -80°C to perform a PST accumulation quantification (Fig. 1).

2.4. Experimental set up for physiological measurements

Experiments were run through a physiological measurement system designed to allow the simultaneous measurements of king scallops respiration and clearance rates (see experimental device described in Flye-Sainte-Marie et al., 2007; Savina and Pouvreau, 2004). Seven king scallop juveniles were each placed into a transparent open-flow 540 mL chamber (n=7) connected to the system. An 8th chamber remained empty, i.e. without any individual, and was used as a control. Chambers were supplied with thermoregulated (ca. 15.7°C) filtered (1 µm) seawater at 35 PSU. Concentrated algal culture was constantly added to the system at the inlet of the ”mixing tank” to reach concentrations between 24 000 and 40 000 cells mL^{-1} and between 440 and 560 cells mL^{-1} for T-iso/Chaeto and *A. minutum* respectively. These concentrations were adjusted as a function of the fluorescence in the control chamber as in Pousse et al., 2018. The seawater inflow was controlled within each chamber by 2 peristaltic pumps placed upstream (each peristaltic pump controlled the seawater flow of 4 chambers) and maintained at a rate of ca. 30 mL min^{-1}. Algal concentrations were measured in the control chamber for each experiment. The 8-tank experimental device is equipped with a multiparameter

probe (WTW MultiLine 3430, Fisher Scientific, Suwanee, GA, USA) measuring both dissolved oxygen and temperature, and a fluorometer (WETstar chlorophyll a, WET Labs, Philomat, USA) quantifying fluorescence in seawater outflow coming from each chamber successively (by alternating control and experimental chambers). Measures lasted 15 min within each chamber with a record every 10 sec. A full set of measurements was thus conducted over 210 min. Real time data could be visualized using a graphical user-interface developed specifically for this system and recorded data were sent to the controller and stored continuously. In order to prevent the development of biofilm that could cause a bias in respiration measurements, the full system was emptied and cleaned with peracetic acid and hydrogen peroxide, rinsed with hot freshwater and then with filtered seawater between the 2 phases of each experimental trial. Juvenile king scallops were kept in filtered seawater during this procedure.

2.5. Physiological parameters

2.5.1. Respiration rate (RR)

The average respiration rate (RR, mg O_2 h^{-1}) of juvenile king scallops was assessed using the following equation:

$$RR = -\left(0_2(control) - 0_2(scallop)\right) \times FR$$

where:

$-0_2(control)$ corresponds to the average oxygen concentration (mg O_2 L^{-1}) in the control chamber recorded prior and after the measurements made in the experimental chamber, and

$-0_2(scallop)$ is the average oxygen concentration (mg O_2 L^{-1}) measured in the experimental chamber and

FR is the seawater flow rate (L h^{-1}) through the chambers.

2.5.2. Clearance rate (CR)

Clearance rate (CR in L h^{-1}) can be defined as the volume of water cleared of particle per unit of time by an individual. Throughout the experiment, seawater outflow from the different chambers was sampled and algal concentration was measured using a Coulter Counter Multisizer. Fluorescence values were converted to cell concentration (cells L^{-1}). CR was calculated as follows:

$$CR = \frac{-\left(FC(control) - FC(scallop)\right)}{FC(control)} \times FR$$

where $FC(control)$ is the average cell concentration (cells L^{-1}) recorded in the control chamber before and after the measurements made in experimental chambers, $FC(scallop)$ corresponds to the average cell concentration (cells L^{-1}) measured in the experimental chamber and FR is the seawater flow rate (L h^{-1}) through the chambers.

Both respiration and clearance rates were standardized using the following equation (Bayne et al., 1987):

$$Y_s = (W_s/W_e)^b \times Y_e.$$

Where Y_s is the physiological rate (respiration or clearance rate in this study) for the standard total mass W_s, Y_e is the physiological rate of the individual that occupied the experimental chamber with a total mass of W_e and b is the allometric coefficient for the clearance (0.67) and respiration (0.75) rates (Bayne et al., 1987). Physiological rates were standardized for a juvenile king scallop with a total mass of 7 g.

Type II linear regressions with range major axis method were applied to adjust linear relationships between the number of consumed algal cells and toxin concentration by using the R package "Lmodel2" (Legendre et al., 2014).

2.5.3. Clearance rate inhibition index (CRII)

The clearance rate inhibition index (CRII) was calculated for each individual, using standardized CR of day 2 (fed with non-toxic algae) and standardized CR of day 4 (exposed to toxic algae). The CRII

was used to quantify CR inhibition due to *A. minutum* and was calculated as follows (Pousse et al., 2018):

$$CRII = 1 - \frac{CR(day2)}{CR(day4)}$$

2.5.4. Time for filtration recovery

The time for filtration recovery was measured from the beginning of *A. minutum* exposure to the time when individual clearance rate reached 0.5 L h^{-1}. This threshold was chosen arbitrarily to detect low levels of filtration activity, without considering erratic filtration behaviors. When individuals CR did not reach this threshold, a time of 40h was applied.

2.6. Toxin accumulation

The PST accumulation was estimated individually using juvenile king scallop digestive gland. HCl was added to digestive gland samples (1:1 w:w) that were then ground using a beadblaster, boiled for 5 min at 104ºC and centrifuged for 10 min. PSTs were subsequently estimated using a Saxitoxin PSP ELISA kit (Abraxis), following instructions from the manufacturer as described in Lassudrie et al. (2014). The acid hydrolysis can induce chemical conversion of some PST analogues to STX (Vale et al., 2008). This Abraxis PSP ELISA assay recognizes mostly STX, and other PSTs only to varying degrees (cross-reactivities of 100% for STX and from 29% to 0% for other PSTs). Thus, toxicity of the digestive glands was expressed as µg of PST per 100 g of wet DG weight.

2.7. Other ecophysiological parameters measured

2.7.1. Toxin accumulation potential

The concentration of toxic algae delivered to king scallops slightly differed in the 3 assays (Fig. 1). Therefore, in order to be able to compare toxin accumulation in all individuals exposed to *A. minutum*, we calculated the toxin accumulation potential of each individual by dividing the toxin concentration

accumulated in digestive glands (DG) at the end of day 4 by the number of *A. minutum* cells distributed during days 3&4 for each individual (µg of PST per 100 g of DG per toxic algal cell delivered).

2.7.2. Number of A. minutum cells consumed (x10^{6} per 100g of DG) and toxins ingested –TI)

From the individual unstandardized CR obtained and the algal concentrations measured in the experimental chambers, the number of *A. minutum* cells consumed can be estimated. To do so, the mean algal concentration (cell L^{-1}) to which a king scallop has been exposed to during a recording cycle (3.5 hours) was multiplied to the unstandardized clearance rate (L h^{-1}) calculated for the corresponding cycle and by 3.5 (h), the duration of each recording cycle. All recording cycles were then added together and divided by the DG mass (g) to obtain the whole quantity of *A. minutum* cells consumed per DG mass during the experiment.

To calculate the overall toxins ingested (TI, µg of STX per 100 g of DG), the number of cells consumed was multiplied by the cellular toxins concentration corresponding to the *A. minutum* strain used in this experiment (52.8x10^{-9} µg STX cell^{-1}).

2.7.3. Toxin accumulation efficiency (TAE)

The toxin accumulation efficiency (TAE) reflects the balance between toxin uptake and elimination processes. It corresponds to the proportion of toxins accumulated (TA, i.e. measured) in king scallop DG during days 3&4 relative to that ingested (TI), and is calculated as follows (Bougrier et al., 2003; Mafra et al., 2010; Pousse et al., 2018):

$$TAE = 100 \times \frac{TA}{TI}$$

2.8. Protein extraction

239 Frozen mantle tissue was crushed with a mixer mill (MM400; RETSCH, Haan, Germany) and kept
240 frozen using liquid nitrogen. For each animal, 100 mg of the obtained mantle tissue powder was
241 homogenized in 100 mM Tris–HCl (pH 6.8) with 1% of protease inhibitor mix (GE Healthcare, Little
242 Chalfont, UK) and centrifuged (50 000 g, 5 min, 4°C). Samples were precipitated overnight at 4°C
243 using TCA 20% (1/1:v/v). After centrifugation (20 000 g, 30 min, 4°C), pellets were washed with
244 70% acetone and re-suspended in thiourea/urea/CHAPS buffer (2 M urea, 7 M thiourea, 4% CHAPS,
245 1% DTT) containing 1% ampholytes (IPG Buffer, pH 4–7; GE Healthcare, Little Chalfont, UK).
246 Protein concentrations were determined using the Bradford derived method and all samples were
247 adjusted to 800 µg of proteins in 250µL.
248
249 *2.9. Two-dimensional electrophoresis (2-DE)*
250 Prior to isoelectric focusing, IPG (immobilized pH gradient) strips (pH 4–7, 13 cm; GE Healthcare,
251 Little Chalfont, UK) were passively rehydrated with 250 µL of protein solution in wells for 14h.
252 Isoelectric focusing was conducted using the following protocol: 250 V for 15 min, 500 V for 2 h,
253 gradient voltage increased to 1000 V for 1 h, gradient voltage increased to 8000 V for 2.5 h, 8000 V
254 for 2 h and finally reduced to 500 V (Ettan IPGphor3; GE Healthcare, Little Chalfont, UK). After
255 isoelectrofocalisation, strips were incubated in equilibration buffer (50 mM Tris–HCl pH 8.8, 6 M
256 urea, 30% glycerol, 2% SDS and 0.002% Bromophenol Blue) for two periods of 15 min, the first one
257 completed with 1 g L^{-1} dithiothreitol and the second time with 48 g L^{-1} iodoacetamide. The IPG strips
258 were then placed on top of 12% polyacrylamide gels (SDS-PAGE) and were run in a 10°C thermo-
259 regulated electrophoresis unit (SE 600 Ruby; Amersham Biosciences, Amersham, UK) at 10 mA per
260 gel for 1 h and then 30 mA per gel until complete migration. Gels were subsequently stained with
261 Coomassie Blue (PhastGel R350, GE Healthcare) and unspecific coloration was destained with an
262 aqueous solution containing 30% methanol and 7% acetic acid. The resulting gels were scanned with
263 a transparency scanner (G:BoxChemi XL 1.4; SynGene) in gray scale with 16-bit depth and a
264 resolution of 100 dpi.

2.10. Gel image and statistical analyzes for protein abundance

Images were aligned and spots were detected and quantified using the Progenesis SameSpots software (version 3.3, Nonlinear Dynamics) with manual alignment completed by automated algorithm. All detected spots were manually checked and artifact spots were removed. Data were exported as raw values and statistical analyzes were conducted in R (R Core Team, 2020) using the prot2D (Artigaud et al., 2013) and limma packages (Ritchie et al., 2015) from the Bioconductor suite (Gentleman et al., 2004). Data were normalized (quantile normalization) and the samples were paired compared between exposed and non-exposed to *A. minutum* conditions using moderated t-test with 7 replicates per condition. For comparisons, we used a moderated t-test, a modified t-test for which the standard errors have been moderated across spots, increasing the reliability of the test (Artigaud et al., 2013). Once the values of moderated t-test were calculated, a global correction by false discovery rate (fdr) was applied, in order to take into account multiple comparisons issues and paired-comparison correction. Spots with a fdr threshold lower than 0.1 and an absolute fold change higher than 1.5 were considered as differentially expressed.

2.11. Mass spectrometry

Proteins that changed significantly in abundance in response to *A. minutum* exposure were excised from gels and prepared for analyzes by mass spectrometry (MS) as described in Artigaud et al., (2015). Gel pieces were washed with 50 mM ammonium bicarbonate (BICAM), dehydrated in 100% acetonitrile (ACN) and vacuum dried. Gel pieces were rehydrated with BICAM containing 0.5 µg of porcine recombinant trypsin (sequencing grade; Promega, Madison, Wisconsin, USA) and incubated overnight at 37°C. Peptides were extracted from the gels by alternative washing with 50 mM BICAM and ACN, and with 5% formic acid and ACN. Between each step, the supernatants were pooled, and finally concentrated by evaporation using a centrifugal evaporator (Concentrator 5301; Eppendorf, Hamburg, Germany).

MS experiments were carried out on an AB Sciex 5800 proteomics analyzer equipped with TOF-TOF ion optics and OptiBeam™ on-axis laser irradiation with 1000 Hz repetition rate. The system was calibrated before analysis with a mixture of des-Arg-bradykinin, angiotensin I, Glu1-fibrinopeptide B, ACTH (18–39) and ACTH (7–38), and mass precision was better than 50 ppm in reflectron mode. A laser intensity of 3400 was typically employed for ionizing. MS spectra were acquired in the positive reflector mode by summarizing 1000 single spectra (5 × 200) in the 700–4000 Da mass range. MS/MS spectra from the twenty most intense ions were acquired in the positive MS/MS reflector mode by summarizing a maximum of 2500 single spectra (10 × 250) with a laser intensity of 4300. For tandem MS experiments, the acceleration voltage was 1 kV, and air was used as the collision gas. Gas pressure medium was selected as settings.

The fragmentation pattern based on the occurrence of y, b and a ions was used to determine peptide sequences. Database searching was performed using the Mascot 2.5.1 program (Matrix Science). A custom EST database was used by combining *P. maximus* sequences from Illumina RNAseq sequenced from mantle tissues (Artigaud et al., 2014) and from hemocyte cells (Pauletto et al., 2014). The variable modifications allowed were as follows: methionine oxidation and dioxidation, acetyl (K) and carbamidomethyl (C). Trypsin was selected as enzyme and 3 missed cleavages were allowed. Mass accuracy was set to 300 ppm and 0.6 Da for the MS and MS/MS modes, respectively.

2.12. Statistical analyzes for toxin accumulation clusters

According to their accumulation potential, individuals were segregated into groups by applying an hierarchical clustering function with the Ward's method (Pousse et al., 2018). The function 'hclust' available in the R package 'stats' (R Core team, 2020) was applied on the accumulation potential calculated for each individual. Three clusters were defined from the clustering function accordingly to Pousse et al. (2018), and Mat et al. (2018) who described phenotypic and genotypic differences in oysters divided into 3 accumulation clusters. This method defined 3 clusters of king scallops

differentially accumulating toxins and named high, medium and low according to their high, intermediate and low accumulation potential, respectively (Fig. 2b).

3. Results

3.1. Inter-individual variability in toxin accumulated and toxin accumulation potential in king scallops exposed to A. minutum.

All king scallops exposed to *A. minutum* for 2 days accumulated toxins and no mortality was observed. For the 3 assays TC-A1, TC-A2 & TC-A3 juvenile king scallops were exposed to different concentrations of *A. minutum* (Fig. 1) allowing us to observe a variation in the toxin loads accumulated ranging from 7 to 220 µg STX per 100 g of DG.

After a 2-day exposure to *A. minutum* toxic algae, our data showed a high variability in toxin accumulation potential between individuals.

Furthermore, according to their accumulation potential, and after applying a hierarchical clustering function with the Ward's method, individuals were segregated into 3 clusters of king scallops differentially accumulating toxins: high (n=5: TC-A1=1, TC-A2=4), intermediate (n=8: TC-A1=3, TC-A2=1, TC-A3=4) and low (n=5: TC-A1=2, TC-A2=2, TC-A3=1) accumulation potential groups (Fig. 2). It is noteworthy that the 3 clusters are irrespective of the 3 replicates.

Within only a 2-day exposure to *A. minutum,* the inter-individual variability in toxin accumulation was high, with an average twice higher in the high accumulation cluster than in the low one.

3.2. Links between feeding behavior and toxin accumulation

Our results demonstrate a significant linear correlation (R^2=0.65) between toxin accumulation in DG and the total numbers of *A. minutum* cells ingested by each king scallop for the 2 days of toxic algae exposure (Fig. 3a).

In all 3 accumulation potential clusters, clearance activity rapidly dropped to almost stop at day 3, when king scallops were exposed to *A. minutum,* and this low clearance rate persisted at day 4 for the

3 clusters (Fig. 3b). Therefore, for all 3 clusters the clearance rates observed during days 3&4 in the presence of *A. minutum* were significantly lower compared to the ones in the presence of non-toxic algae on days 1&2 (p-value<0.005). However, no significant inter-individual difference in clearance rate was observed in the 3 accumulation potential clusters when exposed to toxic algae.

A significant inverse relationship between CRII and the concentration of toxins in king scallop DG (p-value=0.014, Fig. 4a) could be observed. Similar observation was made between CRII and toxin accumulation potential (p-value=0.038, Fig. 4c). No significant correlation could be observed between the CRII and the three different clusters, although a positive trend was visible and should be further analyzed using a higher number of individuals.

Data showed that the time for filtration recovery was positively correlated with the toxin concentrations (p-value=0.014, Fig. 4b), but showed significant inverse relationship with the potential of king scallop to accumulate toxins (p-value=0.002, Fig. 4d). However, King scallop toxin accumulation efficiency (TAE) did not correlate with accumulation potential (Fig. 5).

3.4. Transient inhibition in king scallop respiration rates when exposed to toxic algae A. minutum.

A significantly lower respiration rate was observed on day 3 at the beginning of *A. minutum* exposure compared to *T-iso/C.muelleri* feeding days (days1&2), in correlation to clearance rate results. However, on day 4, in presence of *A. minutum*, the respiration rate came back to its initial level (observed in presence of non-toxic algae during the first 2 days of experiment) (p-value<0.04 ; figure 6a&b). On days 1&2, in presence of non-toxic algae, the respiration rate was not significantly different for the 3 toxin accumulation potential clusters. Similarly, all 3 clusters of king scallops displayed decreased respiration activity on day 3 right after contact with *A. minutum* (less than 4h), and recovered on day 4 (Fig. 6b).

3.5. Proteomic analyzes: differentially accumulated protein spots between king scallops exposed and non-exposed to A. minutum.

In order to complete the above ecophysiological data, the proteomic response was studied by comparing TC-NA (n=7) and TC-A groups (n=7). In total, 13 protein spots were found to be differentially accumulated in the 2-DE gels between *A. minutum* exposed and non-exposed king scallop mantle tissues (Fig. 7). Twelve of the 13 differentially regulated protein spots were successfully identified. They corresponded to 6 different proteins (Table 1). Over the 6 identified proteins, 2 of them displayed higher accumulation levels and 4 were less accumulated in exposed samples, as compared to non-exposed ones. The differentially expressed proteins are involved in cell or tissue structure (beta-actin, filamin A & myosin), in immune response (killer cell lectin-like receptor), energetic metabolism (fructose-bisphosphate aldolase) and detoxification (major vault protein). Several of the identified protein spots appeared as a characteristic horizontal line of spots on the 2-DE electrophoregrams (corresponding to a change in iso-electric point of proteins) as observed for β-actin (spots 8, 9, 10 & 12), paramyosin (spots 2 & 11) and killer cell lectin-like receptor (spots 5 & 6). This may correspond to different phosphorylation states of the proteins (Fig. 7).

4. Discussion

In the present study, both ecophysiological and proteomic approaches were used to study the ecotoxicological response of juvenile king scallops, *P. maximus,* to the toxic microalgae *A. minutum*. High inter-individual variability in toxin accumulation due to feeding behavior has previously been suggested in oysters (Bougrier et al., 2003; Haberkorn et al., 2011; Mat et al., 2013; Pousse et al., 2018). The first aim of this study was to test whether this hypothesis could be expanded to other bivalve species such as *P. maximus*. Here we show that a 2-day exposure to *A. minutum* affects the physiology (behavior and biochemistry) of king scallops. Ecophysiological data highlight 1/ the inter-individual variability in PST accumulation between individual king scallops, linked to feeding behavior; 2/ the *A. minutum* induced inhibition of clearance and of respiration rates, followed by a

recovery; 3/ the influence of level and time for filtration recovery on toxin accumulation. Finally, proteomic data revealed that *A. minutum* exposure caused a differential accumulation in proteins involved in cell/tissue structure, metabolism, detoxification and immune response.

4.1. Physiological effects

4.1.1. Inter-individual variability in king scallops toxin accumulation depends on filter-feeding behavior when exposed to A. minutum.

First of all, we found a significant correlation between toxin accumulation in DG and the total number of *A. minutum* cells ingested by each king scallop. This result suggests that the cells consumed by king scallops during the 2 days of *A. minutum* exposure contributed to the majority of toxin accumulation measured in king scallop DG. Therefore we are confident that toxin accumulation in king scallops is not due to contaminations prior to our experiment. Furthermore, despite their common cohort origin and their identical rearing conditions, a high inter-individual variability in toxin accumulation was found in king scallop juveniles. We cannot exclude that such feature could be due to low numbers of king scallop individuals. However, a high inter-individual variability in toxin accumulation has also been observed in *C. gigas* under controlled laboratory conditions (Mat et al., 2013; Pousse et al., 2018). As for oysters (Boullot et al., 2017; Mat et al., 2018; Pousse et al., 2018), the 3 different profiles in toxin accumulation potential obtained from the Ward's method showed different ecophysiological responses within tested king scallop juveniles. Furthermore, as for oysters and some other tested bivalves (Bougrier et al., 2003; Contreras et al., 2012b; Pousse et al., 2018), we found a correlation between the numbers of toxic algal cells consumed by king scallops and the final toxin concentrations in DG. Our findings also demonstrate that in king scallops, inter-individual differences in toxin accumulation are mainly due to filter-feeding behavior, as observed in several studies on oysters *C. gigas* (Bougrier et al., 2003; Haberkorn et al., 2011; Mat et al., 2018; Pousse et al., 2018). Indeed, when exposed to *A. minutum*, king scallop exhibited inter-individual variability in the time for filtration recovery and the inhibition of clearance rate (CRII) affecting PST accumulation. Such filter-

feeding behavior variability among king scallop individuals toward toxic algae has been observed in several bivalve species (Hégaret et al., 2009; Leverone et al., 2007). As for oysters, we could hypothesize that the high inter-individual variability found among king scallop individuals might be linked to differences in toxin sensitivity (Pousse et al., 2018). More precisely, king scallop toxin accumulation efficiency (TAE), which is another explanatory parameter allowing to understand the inter-individual variability in toxin accumulation was analyzed. Therefore, TAE represents the balance between toxin uptake (i.e. the amount of toxins incorporated) and elimination processes and can depend on pre-ingestion selection, toxin depuration or assimilation (Bougrier et al., 2003; Mafra et al., 2010; Pousse et al., 2018). The TAE values we found for *A. minutum* exposed king scallops (16-59%, average: 32%) are comparable to those calculated for mussels (30-60%, Mafra et al., 2010) and oysters (10-40%, Mafra et al., 2010 and 35%, Pousse et al., 2018) when exposed to *Pseudo-nitzschia* or *A. minutum* for at least 2 days. Species exhibiting high TAE have been suggested to be less sensitive to STX and tend to accumulate it more (For review see Bricelj and Shumway, 1998).

In contrast, this study demonstrated opposite results for *P. maximus* compare to *C. gigas* (Pousse et al., 2018). Indeed, toxin accumulation potential was not influenced by king scallop size/weight or by TAE, which suggests differences in some of the factors influencing toxin accumulation potential among bivalve species. In king scallop, the only factor found to drive toxin accumulation is feeding behavior. Also, in our study, the animal size does not seem to be a factor influencing toxin accumulation. Whereas inter-individual differences in toxin accumulation related to body size have been observed among bivalve species, results similar to our findings have been reported for domoic acid in king scallops (Mafra et al., 2010; Moroño et al., 2001).

4.1.2. Low clearance and respiration activities of king scallops when exposed to toxic A. minutum

As soon as they were exposed to *A. minutum*, all tested king scallops nearly stopped their feeding activity. This reaction toward toxin producing algae has already been highlighted in some, but not all, shellfish species (Contreras et al., 2012b; Hégaret et al., 2009b; Leverone et al., 2007; Pousse et al.,

2018; Seger et al., 2020). Although most of the king scallops re-started filtration again within the 5h following the beginning of *A. minutum* exposure, filtration recovery remained very low in comparison to oysters subjected to similar conditions (Pousse et al., 2018). This result suggests a higher sensitivity of king scallops toward this toxic algae. Coquereau et al (2016) demonstrated indeed that a 2-hour exposure of king scallop to *A. minutum* caused an increase in valve movements, especially closure and expulsion. Similarly, Borcier et al (2017) recorded less filtration and shell growth after immediate exposure to *A. minutum*. Furthermore, Leverone et al. (2007) have shown that among all tested bivalves including eastern oyster (*C. virginica*), northern quahog (*M. mercenaria*) and green mussel (*P. viridis*), the bay scallop *Argopecten irradians,* which is the closest species to king scallop *P. maximus* from this study, was the most sensitive species toward the toxic algae *Karenia brevis* (Leverone et al., 2007). Modification of king scallop feeding behavior was immediate when exposed to toxic algae and this reaction was also observed in oyster (Pousse et al., 2018; Tran et al., 2010). Therefore, rather than a toxin induced response, the avoidance of toxic particles is the most plausible explanation, as suggested in previous studies (Coquereau et al., 2016; Lassus et al., 2004, 1999; Pousse et al., 2018; Wildish et al., 1998).

4.1.3. Toxin accumulation dependence on filtration recovery duration and level

It is now well established that bivalve species, such as oysters, mussels or king scallops have different feeding patterns. Indeed, our findings showing that toxin accumulation efficiency does not influence toxin accumulation in king scallop differs from what has been previously shown in oysters (Pousse et al., 2018). This suggests that there is no clear effects from pre-ingestion mechanisms or toxin absorption/depuration on the inter-individual variability in toxin accumulation profile in king scallop. Our results also highlight that king scallops accumulating more toxins and displaying higher toxin accumulation potential are more likely to start filtration earlier and to exhibit a lower CRII (Fig. 5). This suggests that the high inter-individual variability observed in toxin accumulation due to feeding behavior was driven by two factors: i) the time taken by king scallops to resume filtration after its

inhibition and ii) the level of filtration recovery. Such results have recently been observed in *C. gigas* (Pousse et al., 2018). Therefore, the variability in toxin accumulation due to differential behavior in reducing filtration activity could be a general mechanism in bivalves when facing toxic microalgae, although extra analyzes on other species should be performed to confirm this purpose. In addition, long-term exposure experiments would be necessary to test whether feeding behaviors are still discriminant in toxin accumulation variability. Furthermore, because environmental conditions were the same for all tested individuals, we can reject the assumption of an environmental cause. Therefore, further studies analyzing the mechanisms involved in such inter-individual variabilities, for instance genomic and/or transcriptomic analyzes associated with ecophysiological data, could highlight potential genetic profiles among bivalve species and could link genes to this specific behavior toward toxic algae. In addition, epigenetic variations could also be investigated to determine the factors and mechanisms influencing such differential behavior.

Our data show that respiration rates follow the same evolution as filtration rates until day 3, with a rapid decrease in the presence of toxic algae. However, whereas the filtration profile remains low, the overall respiration activity increases at day 4. Generally, respiration rates increase exponentially with increasing rates of assimilation (Bayne et al., 1989). Comparing the present respiration rates with the feeding rates over the 4-day experiment shows that a decoupling appears to occur at day 4. Respiration rates rises have already been observed in bivalves exposed to environmental stress such as ocean acidification (Pousse et al., 2020), low/high salinity (Peteiro et al., 2018) or toxic algae (Li et al., 2002). In the present context, one hypothesis for this increase in respiration would be that the ingestion of *A. minutum* triggers a metabolic response corresponding to an immune reaction toward the toxic algae and its toxins increasing king scallops respiration rate. It is for instance well known that the consumption of toxic algae by bivalves induces an inflammatory response implying hemocytes degranulation and diapedesis into the digestive tract to encapsulate toxic algae (Galimany et al., 2008; Hégaret et al., 2009a).

4.2. The effects of A. minutum on king scallops at the proteomic level

4.2.1. Cytoskeletal structure

Over the 6 successfully identified proteins, 3 of them are cell structure proteins involved in cytoskeleton composition. It is frequent to find cytoskeletal proteins differentially regulated in proteomic studies because they are highly abundant or conserved proteins among species (Monsinjon and Knigge, 2007). In our study, Filamin A and paramyosin were down regulated, whereas β-actin was upregulated in toxin-exposed king scallops. These 3 proteins are main components of the cytoskeleton orchestrating cell shape, adhesion and motility. More specifically, filamin A cross-links to F-actin proteins, including β-actin, giving to the cells a dynamic three-dimensional structure (Nakamura et al., 2011; Popowicz et al., 2006; Stossel et al., 2001). Therefore, modifications of cytoskeleton composition in toxin-exposed mantle cells may depict a cytoskeleton disintegration or restructuration. It is now well established that several phycotoxins display toxicity toward cytoskeleton, especially actin. Indeed, the main molecular target of several microalgal toxins is cytoskeleton. *In vitro* studies have demonstrated that pectonotoxin-2 was disrupting actin organization in several cell types (Spector et al., 1999). Furthermore, DSP toxins such as okadaic acid have also been reported to disturb cytoskeleton dynamic and integrity in several organisms including bivalves (Huang et al., 2015; Vilariño et al., 2008; Yoon et al., 2008). Furthermore, Hégaret et al. (2007) observed adductor-muscle paralysis in some oysters *Crassostrea virginica* exposed to another PST producer, *Alexandrium fundyense,* which could be related to cytoskeleton mis-functioning. Muscular contraction is an important pathway related to digestion that appeared affected by toxins. Indeed, Mat et al. (2018) also observed over-expression of calmodulin, which regulates binding between myosin and actin in smooth muscles, whereas the muscarinic acetylcholine receptor (M3R), important in the contractile response in smooth muscle, particularly in gastrointestinal smooth muscles, was down-regulated in *C. gigas* with high PST loads (Mat et al., 2018).

4.2.2. Detoxification

Even though no correspondence could be clearly established between toxin accumulation profiles and proteomic analyzes, mass spectrometry results brought insights on the functioning of ecotoxicological response. Firstly, not surprising in toxin-challenged experiments, a protein involved in detoxification was identified. The Major Vault Protein (MVP) is the main component of ribonucleoprotein particles called vault (Tanaka et al., 2009). Vaults were suggested to be involved in signaling, innate immunity and detoxification (Berger et al., 2009). In particular, MVP is considered as a major multidrug resistance protein since several studies have found high expression of MVP correlated with chemotherapy resistance (Kickhoefer et al., 1998; Scheper et al., 1993). Additional studies have demonstrated that MVP could have a role in drug molecule export from nucleus to cytoplasmic vesicles for sequestration (Herlevsen et al., 2007; Suprenant et al., 2007). Furthermore, other proteomic studies have shown an increase of MVP in mussel, *Mytilus galloprovincialis*, when exposed to aquatic pollutants such as Ag nanoparticles or a mixture of Cu and benzo(a)pyrene (Gomes et al., 2013; Maria et al., 2013). Therefore, it appears that MVP would be involved in xenobiotic detoxification. Surprisingly in our case, MVP is decreased when king scallops are exposed to PST producing *A. minutum*, which suggests that there might be a mechanism blocking the MVP-dependent detoxification pathway. Possibly, *A. minutum* could be responsible for this blockage by secretion of molecules inhibiting detoxification pathways. Similar to our results, Tomanek and Zuzow have found a lower abundance of two isoforms of VMP in *Mytilus galloprovincialis* subjected to temperature stress and have suggested that it could be part of an antiapoptotic response (Tomanek and Zuzow, 2010), therefore corresponding to a more general stress response rather than a specific detoxification process.

4.2.3. Glycolysis balance

The fructose-bisphosphate aldolase is one of the major proteins involved in glycolysis and gluconeogenesis pathways. In our study we found a lower concentration of fructose-bisphosphate aldolase in king scallops exposed to *A. minutum* than in the control group. This result suggests a

subsequent decrease of glycolysis in mantle tissue of PST challenged king scallops due to the accumulation of toxins in this tissue. Lower levels of fructose-bisphosphate aldolase have been found in the kuruma prawn, *Marsupenaeus japonicus*, under stressful, hypoxic conditions (Abe et al., 2007). In the same way, it is possible that glycolysis in king scallop is down-regulated when exposed to cytotoxic *A. minutum*. In another hand, transcriptomic studies have shown higher amounts of fructose-bisphosphate aldolase transcripts in oyster exhibiting higher toxin accumulation (Mat et al., 2018). Here again, there might be differences in metabolic responses against toxic algae exposure within bivalves species. This opposite result could also come from differences in the experimental design (as described above) suggesting that the age of animals or the BEC could have an impact on the metabolic response.

4.2.4. Immune system regulation

Finally, we show that the killer cell lectin-like receptor subfamily B member 1B (KLRB1B also called NKR-P1B) is more abundantly accumulated in *A. minutum* exposed king scallops. The NKR-P1B is part of the receptor family regulating the cytotoxic activity of Natural Killer cells (NK). NK cells are sentinels focused on the early detection of pathogens and their inhibitory receptor NKR-P1B plays a key role in protecting healthy tissues from NK cell-mediated lysis (Balaji et al., 2018). NKR-P1B is specifically expressed on the surface of NK cells in animals possessing adaptive immunity. Whereas no adaptive immunity has been described in bivalves, several studies have demonstrated that blue mussel previously exposed to toxic microalgae accumulated less PST than the ones exposed for the first time (Shumway and Cucci, 1987). In the same way, recent studies have suggested the existence of an immune memory in oysters (Lafont et al., 2019, 2017). Furthermore, Araya and collaborators have shown the presence of NKR in hemocytes of soft-shell clams, *Mya arenaria*, suggesting a potential cytotoxic activity from hemocytes (Araya et al., 2010). Other studies have also observed cytotoxic activity in blue mussel, *Mytilus edulis,* suggesting that hemocytes may act as NK cells (Hannam et al., 2009). Our findings that NKR-P1B is more abundant in toxic algae exposed king scallops

suggest a down-regulation of the hemocyte cytotoxic activity through specific receptors. Very little is known about receptor mediated immune response and their corresponding intracellular signaling pathways in bivalves. Further research at the molecular level would allow to better characterize receptors, signaling molecules and pathways orchestrating the immune response in order to better understand the mechanisms regulating the cytotoxic activity found in bivalves.

5. Conclusion

Our data show for the first time that juvenile king scallops *P. maximus* have an important inter-individual variability in toxin accumulation driven by its feeding behavior. Our study further highlights the effects of delay and level for filtration recovery on toxin accumulation in king scallops. Furthermore, proteomic analyzes suggest an effect of toxic algae *A. minutum* on immune response, cytoskeleton remodeling, detoxication and metabolism of king scallops.

Conflict of Interest Disclosures

The authors declare no competing financial interests.

Acknowledgements

This project was supported by the National Research Agency ANR CESA (ACCUTOX project ANR-13-CESA-0019). Coraline Chapperon was supported by a postdoctoral fellowship from the Conseil Départemental du Finistère. The authors gratefully acknowledge Isabelle Quéau and Adeline Bidault who provided technical help for ecophysiological and proteomic experiments.

Author contributions

YE, EP, SA & CC: Collection and/or assembly of data, data analyzes and interpretation, manuscript writing. HH: Conception and design, financial support, manuscript writing. VP: financial support, manuscript writing. JFSM: Conception and design. FJ: financial support.

References

Abe, H., Hirai, S., Okada, S., 2007. Metabolic responses and arginine kinase expression under hypoxic stress of the kuruma prawn Marsupenaeus japonicus. Comp. Biochem. Physiol. A. Mol. Integr. Physiol. 146, 40–46. https://doi.org/10.1016/j.cbpa.2006.08.027

Anderson, D.M., Alpermann, T.J., Cembella, A.D., Collos, Y., Masseret, E., Montresor, M., 2012. The globally distributed genus Alexandrium: Multifaceted roles in marine ecosystems and impacts on human health. Harmful Algae, Harmful Algae--The requirement for species-specific information 14, 10–35. https://doi.org/10.1016/j.hal.2011.10.012

Araya, M.T., Markham, F., Mateo, D.R., McKenna, P., Johnson, G.R., Berthe, F.C.J., Siah, A., 2010. Identification and expression of immune-related genes in hemocytes of soft-shell clams, Mya arenaria, challenged with Vibrio splendidus. Fish Shellfish Immunol. 29, 557–564. https://doi.org/10.1016/j.fsi.2010.05.017

Artigaud, S., Gauthier, O., Pichereau, V., 2013. Identifying differentially expressed proteins in two-dimensional electrophoresis experiments: inputs from transcriptomics statistical tools. Bioinformatics 29, 2729–2734. https://doi.org/10.1093/bioinformatics/btt464

Artigaud, S., Lacroix, C., Richard, J., Flye-Sainte-Marie, J., Bargelloni, L., Pichereau, V., 2015. Proteomic responses to hypoxia at different temperatures in the great scallop (Pecten maximus). PeerJ 3, e871. https://doi.org/10.7717/peerj.871

Artigaud, S., Thorne, M.A.S., Richard, J., Lavaud, R., Jean, F., Flye-Sainte-Marie, J., Peck, L.S., Pichereau, V., Clark, M.S., 2014. Deep sequencing of the mantle transcriptome of the great scallop Pecten maximus. Mar. Genomics 15, 3–4. https://doi.org/10.1016/j.margen.2014.03.006

Baird, R.H., 1958. Measurement of Condition in Mussels and Oysters. ICES J. Mar. Sci. 23, 249–257. https://doi.org/10.1093/icesjms/23.2.249

Balaji, G.R., Aguilar, O.A., Tanaka, M., Shingu-Vazquez, M.A., Fu, Z., Gully, B.S., Lanier, L.L., Carlyle, J.R., Rossjohn, J., Berry, R., 2018. Recognition of host Clr-b by the inhibitory NKR-P1B receptor provides a basis for missing-self recognition. Nat. Commun. 9, 4623. https://doi.org/10.1038/s41467-018-06989-2

Bayne, B.L., Hawkins, A.J.S., Navarro, E., 1987. Feeding and digestion by the mussel Mytilus edulis L. (Bivalvia: Mollusca) in mixtures of silt and algal cells at low concentrations. J. Exp. Mar. Biol. Ecol. 111, 1–22. https://doi.org/10.1016/0022-0981(87)90017-7

Bayne, B.L., Hawkins, A.J.S., Navarro, E., Iglesias, I.P., 1989. Effects of seston concentration on feeding, digestion and growth in the mussel Mytilus edulis. Mar. Ecol. Prog. Ser. 55, 47–54.

Berger, W., Steiner, E., Grusch, M., Elbling, L., Micksche, M., 2009. Vaults and the major vault protein: Novel roles in signal pathway regulation and immunity. Cell. Mol. Life Sci. 66, 43–61. https://doi.org/10.1007/s00018-008-8364-z

Borcier, E., Morvezen, R., Boudry, P., Miner, P., Charrier, G., Laroche, J., Hegaret, H., 2017. Effects of bioactive extracellular compounds and paralytic shellfish toxins produced by Alexandrium minutum on growth and behaviour of juvenile great scallops Pecten maximus. Aquat. Toxicol. 184, 142–154. https://doi.org/10.1016/j.aquatox.2017.01.009

Bougrier, S., Lassus, P., Bardouil, M., Masselin, P., Truquet, P., 2003. Paralytic shellfish poison accumulation yields and feeding time activity in the Pacific oyster (Crassostrea gigas) and king scallop (Pecten maximus). Aquat. Living Resour. 16, 347–352. https://doi.org/10.1016/S0990-7440(03)00080-9

Boullot, F., Castrec, J., Bidault, A., Dantas, N., Payton, L., Perrigault, M., Tran, D., Amzil, Z., Boudry, P., Soudant, P., Hégaret, H., Fabioux, C., 2017. Molecular Characterization of Voltage-

Gated Sodium Channels and Their Relations with Paralytic Shellfish Toxin Bioaccumulation in the Pacific Oyster Crassostrea gigas. Mar. Drugs 15, 21. https://doi.org/10.3390/md15010021

Bricelj, V.M., Shumway, S.E., 1998. Paralytic Shellfish Toxins in Bivalve Molluscs: Occurrence, Transfer Kinetics, and Biotransformation. Rev. Fish. Sci. 6, 315–383. https://doi.org/10.1080/10641269891314294

Castrec, J., Hégaret, H., Alunno-Bruscia, M., Picard, M., Soudant, P., Petton, B., Boulais, M., Suquet, M., Quéau, I., Ratiskol, D., Foulon, V., Le Goïc, N., Fabioux, C., 2019. The dinoflagellate Alexandrium minutum affects development of the oyster Crassostrea gigas, through parental or direct exposure. Environ. Pollut. 246, 827–836. https://doi.org/10.1016/j.envpol.2018.11.084

Castrec, J., Soudant, P., Payton, L., Tran, D., Miner, P., Lambert, C., Le Goïc, N., Huvet, A., Quillien, V., Boullot, F., Amzil, Z., Hégaret, H., Fabioux, C., 2018. Bioactive extracellular compounds produced by the dinoflagellate Alexandrium minutum are highly detrimental for oysters. Aquat. Toxicol. 199, 188–198. https://doi.org/10.1016/j.aquatox.2018.03.034

Chauvaud, L., Donval, A., Thouzeau, G., Paulet, Y.-M., Nézan, E., 2001. Variations in food intake of Pecten maximus (L.) from the Bay of Brest (France): Influence of environmental factors and phytoplankton species composition. Comptes Rendus Académie Sci. - Ser. III - Sci. Vie 324, 743–755. https://doi.org/10.1016/S0764-4469(01)01349-X

Chauvaud, L., Thouzeau, G., Paulet, Y.-M., 1998. Effects of environmental factors on the daily growth rate of Pecten maximus juveniles in the Bay of Brest (France). J. Exp. Mar. Biol. Ecol. 227, 83–111. https://doi.org/10.1016/S0022-0981(97)00263-3

Contreras, A.M., Marsden, I.D., Munro, M.H.G., 2012a. Physiological Effects and Biotransformation of PSP Toxins in the New Zealand Scallop, Pecten novaezelandiae. J. Shellfish Res. 31, 1151–1159. https://doi.org/10.2983/035.031.0426

Contreras, A.M., Marsden, I.D., Munro, M.H.G., 2012b. Effects of short-term exposure to paralytic shellfish toxins on clearance rates and toxin uptake in five species of New Zealand bivalve. Mar. Freshw. Res. 63, 166–174. https://doi.org/10.1071/MF11173

Coquereau, L., Jolivet, A., Hégaret, H., Chauvaud, L., 2016. Short-Term Behavioural Responses of the Great Scallop Pecten maximus Exposed to the Toxic Alga Alexandrium minutum Measured by Accelerometry and Passive Acoustics. PLOS ONE 11, e0160935. https://doi.org/10.1371/journal.pone.0160935

Fabioux, C., Sulistiyani, Y., Haberkorn, H., Hégaret, H., Amzil, Z., Soudant, P., 2015. Exposure to toxic Alexandrium minutum activates the detoxifying and antioxidant systems in gills of the oyster Crassostrea gigas. Harmful Algae 48, 55–62. https://doi.org/10.1016/j.hal.2015.07.003

FAO Fisheries and Aquaculture Department - Yearbook of Fishery and Aquaculture Statistics - Capture production [WWW Document], n.d. URL https://www.fao.org/fishery/static/Yearbook/YB2019_USBcard/navigation/index_content_capture_e.htm (accessed 1.10.22).

Flye-Sainte-Marie, J., Pouvreau, S., Paillard, C., Jean, F., 2007. Impact of Brown Ring Disease on the energy budget of the Manila clam Ruditapes philippinarum. J. Exp. Mar. Biol. Ecol. 349, 378–389. https://doi.org/10.1016/j.jembe.2007.05.029

Galimany, E., Sunila, I., Hégaret, H., Ramón, M., Wikfors, G.H., 2008. Experimental exposure of the blue mussel (Mytilus edulis, L.) to the toxic dinoflagellate Alexandrium fundyense: Histopathology, immune responses, and recovery. Harmful Algae 7, 702–711. https://doi.org/10.1016/j.hal.2008.02.006

Gentleman, R.C., Carey, V.J., Bates, D.M., Bolstad, B., Dettling, M., Dudoit, S., Ellis, B., Gautier, L., Ge, Y., Gentry, J., Hornik, K., Hothorn, T., Huber, W., Iacus, S., Irizarry, R., Leisch, F., Li, C., Maechler, M., Rossini, A.J., Sawitzki, G., Smith, C., Smyth, G., Tierney, L., Yang, J.Y., Zhang, J., 2004. Bioconductor: open software development for computational biology and bioinformatics. Genome Biol. 5, R80. https://doi.org/10.1186/gb-2004-5-10-r80

Geraci, J.R., Anderson, D.M., Timperi, R.J., St. Aubin, D.J., Early, G.A., Prescott, J.H., Mayo, C.A., 1989. Humpback Whales (Megaptera novaeangliae) Fatally Poisoned by Dinoflagellate Toxin. Can. J. Fish. Aquat. Sci. 46, 1895–1898. https://doi.org/10.1139/f89-238

Gomes, T., Pereira, C.G., Cardoso, C., Bebianno, M.J., 2013. Differential protein expression in mussels Mytilus galloprovincialis exposed to nano and ionic Ag. Aquat. Toxicol. 136–137, 79–90. https://doi.org/10.1016/j.aquatox.2013.03.021

Guillard, R.R.L., Hargraves, P.E., 1993. Stichochrysis immobilis is a diatom, not a chrysophyte. Phycologia 32, 234–236. https://doi.org/10.2216/i0031-8884-32-3-234.1

Haberkorn, H., Lambert, C., Le Goïc, N., Guéguen, M., Moal, J., Palacios, E., Lassus, P., Soudant, P., 2010a. Effects of Alexandrium minutum exposure upon physiological and hematological variables of diploid and triploid oysters, Crassostrea gigas. Aquat. Toxicol. 97, 96–108. https://doi.org/10.1016/j.aquatox.2009.12.006

Haberkorn, H., Lambert, C., Le Goïc, N., Moal, J., Suquet, M., Guéguen, M., Sunila, I., Soudant, P., 2010b. Effects of Alexandrium minutum exposure on nutrition-related processes and reproductive output in oysters Crassostrea gigas. Harmful Algae 9, 427–439. https://doi.org/10.1016/j.hal.2010.01.003

Haberkorn, H., Tran, D., Massabuau, J.-C., Ciret, P., Savar, V., Soudant, P., 2011. Relationship between valve activity, microalgae concentration in the water and toxin accumulation in the digestive gland of the Pacific oyster Crassostrea gigas exposed to Alexandrium minutum. Mar. Pollut. Bull. 62, 1191–1197. https://doi.org/10.1016/j.marpolbul.2011.03.034

Hannam, M.L., Bamber, S.D., Sundt, R.C., Galloway, T.S., 2009. Immune modulation in the blue mussel Mytilus edulis exposed to North Sea produced water. Environ. Pollut. 157, 1939–1944. https://doi.org/10.1016/j.envpol.2008.12.031

Hégaret, Hélène, da Silva, P.M., Sunila, I., Shumway, S.E., Dixon, M.S., Alix, J., Wikfors, G.H., Soudant, P., 2009a. Perkinsosis in the Manila clam Ruditapes philippinarum affects responses to the harmful-alga, Prorocentrum minimum. J. Exp. Mar. Biol. Ecol. 371, 112–120. https://doi.org/10.1016/j.jembe.2009.01.016

Hégaret, Hélène, Wikfors, G., Shumway, S., 2009b. Diverse feeding responses of five species of bivalve mollusc when exposed to three species of harmful algae. J. Shellfish Res. 26, 549–559. https://doi.org/10.2983/0730-8000(2007)26[549:DFROFS]2.0.CO;2

Hégaret, H., Wikfors, G.H., Shumway, S. E., 2009. 2 - Biotoxin contamination and shellfish safety, in: Shumway, Sandra E., Rodrick, G.E. (Eds.), Shellfish Safety and Quality, Woodhead Publishing Series in Food Science, Technology and Nutrition. Woodhead Publishing, pp. 43–80. https://doi.org/10.1533/9781845695576.1.43

Hégaret, H., Wikfors, G.H., Soudant, P., Lambert, C., Shumway, S.E., Bérard, J.B., Lassus, P., 2007. Toxic dinoflagellates (Alexandriumfundyense and A. catenella) have minimal apparent effects on oyster hemocytes. Mar. Biol. 152, 441–447. https://doi.org/10.1007/s00227-007-0703-3

Herlevsen, M., Oxford, G., Owens, C.R., Conaway, M., Theodorescu, D., 2007. Depletion of major vault protein increases doxorubicin sensitivity and nuclear accumulation and disrupts its sequestration in lysosomes. Mol. Cancer Ther. 6, 1804–1813. https://doi.org/10.1158/1535-7163.MCT-06-0372

Huang, L., Zou, Y., Weng, H., Li, H.-Y., Liu, J.-S., Yang, W.-D., 2015. Proteomic profile in Perna viridis after exposed to Prorocentrum lima, a dinoflagellate producing DSP toxins. Environ. Pollut. 196, 350–357. https://doi.org/10.1016/j.envpol.2014.10.019

Kickhoefer, V.A., Rajavel, K.S., Scheffer, G.L., Dalton, W.S., Scheper, R.J., Rome, L.H., 1998. Vaults Are Up-regulated in Multidrug-resistant Cancer Cell Lines. J. Biol. Chem. 273, 8971–8974. https://doi.org/10.1074/jbc.273.15.8971

Lafont, M., Goncalves, P., Guo, X., Montagnani, C., Raftos, D., Green, T., 2019. Transgenerational plasticity and antiviral immunity in the Pacific oyster (Crassostrea gigas) against Ostreid

herpesvirus 1 (OsHV-1). Dev. Comp. Immunol. 91, 17–25. https://doi.org/10.1016/j.dci.2018.09.022

Lafont, M., Petton, B., Vergnes, A., Pauletto, M., Segarra, A., Gourbal, B., Montagnani, C., 2017. Long-lasting antiviral innate immune priming in the Lophotrochozoan Pacific oyster, Crassostrea gigas. Sci. Rep. 7, 13143. https://doi.org/10.1038/s41598-017-13564-0

Lassudrie, M., Soudant, P., Richard, G., Henry, N., Medhioub, W., da Silva, P.M., Donval, A., Bunel, M., Le Goïc, N., Lambert, C., de Montaudouin, X., Fabioux, C., Hégaret, H., 2014. Physiological responses of Manila clams Venerupis (=Ruditapes) philippinarum with varying parasite Perkinsus olseni burden to toxic algal Alexandrium ostenfeldii exposure. Aquat. Toxicol. 154, 27–38. https://doi.org/10.1016/j.aquatox.2014.05.002

Lassus, P., Bardouil, M., Beliaeff, B., Masselin, P., Naviner, M., Truquet, P., 1999. Effect of a continuous supply of the toxic dinoflagellate Alexandrium minutum halim on the feeding behavior of the pacific oyster (Crassostrea gigas thunberg). J. Shellfish Res. 18, 211–216.

Lassus, P., Baron, R., Garen, P., Truquet, P., Masselin, P., Bardouil, M., Leguay, D., Amzil, Z., 2004. Paralytic shellfish poison outbreaks in the Penzé estuary: Environmental factors affecting toxin uptake in the oyster, Crassostrea gigas. Aquat. Living Resour. 17, 207–214. https://doi.org/10.1051/alr:2004012

Legendre, P., 2014. Lmodel2: Model II Regression. R Package Version 1.7-2 [WWW Document]. URL http://CRAN.R-project.org/package=lmodel2 (accessed 11.15.19).

Leverone, J.R., Shumway, S.E., Blake, N.J., 2007. Comparative effects of the toxic dinoflagellate Karenia brevis on clearance rates in juveniles of four bivalve molluscs from Florida, USA. Toxicon 49, 634–645. https://doi.org/10.1016/j.toxicon.2006.11.003

Li, S.-C., Wang, W.-X., Hsieh, D.P.H., 2002. Effects of toxic dinoflagellate Alexandrium tamarense on the energy budgets and growth of two marine bivalves. Mar. Environ. Res. 53, 145–160. https://doi.org/10.1016/S0141-1136(01)00117-9

Long, M., Tallec, K., Soudant, P., Le Grand, F., Donval, A., Lambert, C., Sarthou, G., Jolley, D.F., Hégaret, H., 2018. Allelochemicals from Alexandrium minutum induce rapid inhibition of metabolism and modify the membranes from Chaetoceros muelleri. Algal Res. 35, 508–518. https://doi.org/10.1016/j.algal.2018.09.023

Mafra, L.L., Bricelj, V.M., Fennel, K., 2010. Domoic acid uptake and elimination kinetics in oysters and mussels in relation to body size and anatomical distribution of toxin. Aquat. Toxicol. 100, 17–29. https://doi.org/10.1016/j.aquatox.2010.07.002

Maria, V.L., Gomes, T., Barreira, L., Bebianno, M.J., 2013. Impact of benzo(a)pyrene, Cu and their mixture on the proteomic response of Mytilus galloprovincialis. Aquat. Toxicol. 144–145, 284–295. https://doi.org/10.1016/j.aquatox.2013.10.009

Mat, A.M., Haberkorn, H., Bourdineaud, J.-P., Massabuau, J.-C., Tran, D., 2013. Genetic and genotoxic impacts in the oyster Crassostrea gigas exposed to the harmful alga Alexandrium minutum. Aquat. Toxicol. 140–141, 458–465. https://doi.org/10.1016/j.aquatox.2013.07.008

Mat, A.M., Klopp, C., Payton, L., Jeziorski, C., Chalopin, M., Amzil, Z., Tran, D., Wikfors, G.H., Hégaret, H., Soudant, P., Huvet, A., Fabioux, C., 2018. Oyster transcriptome response to Alexandrium exposure is related to saxitoxin load and characterized by disrupted digestion, energy balance, and calcium and sodium signaling. Aquat. Toxicol. 199, 127–137. https://doi.org/10.1016/j.aquatox.2018.03.030

Monsinjon, T., Knigge, T., 2007. Proteomic applications in ecotoxicology. PROTEOMICS 7, 2997–3009. https://doi.org/10.1002/pmic.200700101

Moroño, A., Franco, J., Miranda, M., Reyero, M.I., Blanco, J., 2001. The effect of mussel size, temperature, seston volume, food quality and volume-specific toxin concentration on the uptake rate of PSP toxins by mussels (Mytilus galloprovincialis Lmk). J. Exp. Mar. Biol. Ecol. 257, 117–132. https://doi.org/10.1016/S0022-0981(00)00336-1

Nakamura, F., Stossel, T.P., Hartwig, J.H., 2011. The filamins. Cell Adhes. Migr. 5, 160–169. https://doi.org/10.4161/cam.5.2.14401

Narahashi, T., Moore, J.W., 1968. Neuroactive agents and nerve membrane conductances. J. Gen. Physiol. 51, 93.

Pauletto, M., Milan, M., Moreira, R., Novoa, B., Figueras, A., Babbucci, M., Patarnello, T., Bargelloni, L., 2014. Deep transcriptome sequencing of Pecten maximus hemocytes: A genomic resource for bivalve immunology. Fish Shellfish Immunol. 37, 154–165. https://doi.org/10.1016/j.fsi.2014.01.017

Payton, L., Perrigault, M., Hoede, C., Massabuau, J.-C., Sow, M., Huvet, A., Boullot, F., Fabioux, C., Hegaret, H., Tran, D., 2017. Remodeling of the cycling transcriptome of the oyster Crassostrea gigas by the harmful algae Alexandrium minutum. Sci. Rep. 7. https://doi.org/10.1038/s41598-017-03797-4

Peteiro, L.G., Woodin, S.A., Wethey, D.S., Costas-Costas, D., Martínez-Casal, A., Olabarria, C., Vázquez, E., 2018. Responses to salinity stress in bivalves: Evidence of ontogenetic changes in energetic physiology on Cerastoderma edule. Sci. Rep. 8, 8329. https://doi.org/10.1038/s41598-018-26706-9

Popowicz, G.M., Schleicher, M., Noegel, A.A., Holak, T.A., 2006. Filamins: promiscuous organizers of the cytoskeleton. Trends Biochem. Sci. 31, 411–419. https://doi.org/10.1016/j.tibs.2006.05.006

Pousse, É., Flye-Sainte-Marie, J., Alunno-Bruscia, M., Hégaret, H., Jean, F., 2018. Sources of paralytic shellfish toxin accumulation variability in the Pacific oyster Crassostrea gigas. Toxicon 144, 14–22. https://doi.org/10.1016/j.toxicon.2017.12.050

Pousse, E., Poach, M.E., Redman, D.H., Sennefelder, G., White, L.E., Lindsay, J.M., Munroe, D., Hart, D., Hennen, D., Dixon, M.S., Li, Y., Wikfors, G.H., Meseck, S.L., 2020. Energetic response of Atlantic surfclam Spisula solidissima to ocean acidification. Mar. Pollut. Bull. 161, 111740. https://doi.org/10.1016/j.marpolbul.

R Core Team, 2020. R: A language and environment for statistical computing. R Foundation for Statistical Computing, Vienna, Austria. http://www.R-project.org.

Reyero, M., Cacho, E., Martínez, A., Vázquez, J., Marina, A., Fraga, S., Franco, J.M., 1999. Evidence of saxitoxin derivatives as causative agents in the 1997 mass mortality of monk seals in the Cape Blanc Peninsula. Nat. Toxins 7, 311–315. https://doi.org/10.1002/1522-7189(199911/12)7:6<311::AID-NT75>3.0.CO;2-I

Ritchie, J.M., Rogart, R.B., 1977. The binding of saxitoxin and tetrodotoxin to excitable tissue, in: Reviews of Physiology, Biochemistry and Pharmacology, Volume 79. Springer, pp. 1–50.

Ritchie, M.E., Phipson, B., Wu, D., Hu, Y., Law, C.W., Shi, W., Smyth, G.K., 2015. limma powers differential expression analyses for RNA-sequencing and microarray studies. Nucleic Acids Res. 43, e47–e47. https://doi.org/10.1093/nar/gkv007

Savina, M., Pouvreau, S., 2004. A comparative ecophysiological study of two infaunal filter-feeding bivalves: Paphia rhomboïdes and Glycymeris glycymeris. Aquaculture 239, 289–306. https://doi.org/10.1016/j.aquaculture.2004.05.029

Scheper, R.J., Broxterman, H.J., Scheffer, G.L., Kaaijk, P., Dalton, W.S., van Heijningen, T.H., van Kalken, C.K., Slovak, M.L., de Vries, E.G., van der Valk, P., 1993. Overexpression of a M(r) 110,000 vesicular protein in non-P-glycoprotein-mediated multidrug resistance. Cancer Res. 53, 1475–1479.

Seger, A., Hallegraeff, G., Stone, D.A.J., Bansemer, M.S., Harwood, D.T., Turnbull, A., 2020. Uptake of Paralytic Shellfish Toxins by Blacklip Abalone (Haliotis rubra rubra Leach) from direct exposure to Alexandrium catenella microalgal cells and toxic aquaculture feed. Harmful Algae 99, 101925. https://doi.org/10.1016/j.hal.2020.101925

Shumway, S.E., Cucci, T.L., 1987. The effects of the toxic dinoflagellate Protogonyaulax tamarensis on the feeding and behaviour of bivalve molluscs. Aquat. Toxicol. 10, 9–27. https://doi.org/10.1016/0166-445X(87)90024-5

Spector, I., Braet, F., Shochet, N.R., Bubb, M.R., 1999. New anti-actin drugs in the study of the organization and function of the actin cytoskeleton. Microsc. Res. Tech. 47, 18–37. https://doi.org/10.1002/(SICI)1097-0029(19991001)47:1<18::AID-JEMT3>3.0.CO;2-E

Stossel, T.P., Condeelis, J., Cooley, L., Hartwig, J.H., Noegel, A., Schleicher, M., Shapiro, S.S., 2001. Filamins as integrators of cell mechanics and signalling. Nat. Rev. Mol. Cell Biol. 2, 138–145. https://doi.org/10.1038/35052082

Suprenant, K.A., Bloom, N., Fang, J., Lushington, G., 2007. The major vault protein is related to the toxic anion resistance protein (TelA) family. J. Exp. Biol. 210, 946–955. https://doi.org/10.1242/jeb.001800

Tanaka, H., Kato, K., Yamashita, E., Sumizawa, T., Zhou, Y., Yao, M., Iwasaki, K., Yoshimura, M., Tsukihara, T., 2009. The Structure of Rat Liver Vault at 3.5 Angstrom Resolution 323, 5.

Tomanek, L., Zuzow, M.J., 2010. The proteomic response of the mussel congeners Mytilus galloprovincialis and M. trossulus to acute heat stress: implications for thermal tolerance limits and metabolic costs of thermal stress. J. Exp. Biol. 213, 3559–3574. https://doi.org/10.1242/jeb.041228

Tran, D., Haberkorn, H., Soudant, P., Ciret, P., Massabuau, J.-C., 2010. Behavioral responses of Crassostrea gigas exposed to the harmful algae Alexandrium minutum. Aquaculture 298, 338–345. https://doi.org/10.1016/j.aquaculture.2009.10.030

Vale, C., Alfonso, A., Vieytes, M.R., Romarís, X.M., Arévalo, F., Botana, A.M., Botana, L.M., 2008. In Vitro and in Vivo Evaluation of Paralytic Shellfish Poisoning Toxin Potency and the Influence of the pH of Extraction. Anal. Chem. 80, 1770–1776. https://doi.org/10.1021/ac7022266

Vilariño, N., Ares, I.R., Cagide, E., Louzao, M.C., Vieytes, M.R., Yasumoto, T., Botana, L.M., 2008. Induction of actin cytoskeleton rearrangement by methyl okadaate – comparison with okadaic acid. FEBS J. 275, 926–934. https://doi.org/10.1111/j.1742-4658.2008.06256.x

Walne, P.R., 1970. Studies on the food value of nineteen genera of algae to juvenile bivalves of the genera Ostrea, Crassostrea, Mercenaria and Mytilus. Fish Invest Ser 2 26.

Walne, P.R., 1966. Experiments in the large-scale culture of the larvae of Ostrea edulis L. H. M. Stationery Off.

Wildish, D., Lassus, P., Martin, J., Saulnier, A., Bardouil, M., 1998. Effect of the PSP-causing dinoflagellate, Alexandrium sp. on the initial feeding response of Crassostrea gigas. Aquat. Living Resour. 11, 35–43. https://doi.org/10.1016/S0990-7440(99)80029-1

Yoon, S.Y., Choi, J.E., Choi, J.M., Kim, D.H., 2008. Dynein cleavage and microtubule accumulation in okadaic acid-treated neurons. Neurosci. Lett. 437, 111–115. https://doi.org/10.1016/j.neulet.2008.03.083

Figures

Figure 1: Scheme depicting the experimental design.

For each condition, 7 biological replicates were collected. T-iso: *Tisochrisis lutea,* C: *Chaetoceros muelleri*. Group TC-NA corresponds to scallops exposed to T-iso&C for days 1&2, and without algae for days 3&4 (n=7). Groups TC-A correspond to scallops exposed to T-iso&C for days 1&2 and to *A. minutum* for days 3&4 (n=18).

Figure 2: Interindividual variability of toxin accumulation potential

Accumulation potential corresponding to the ratio between final toxin content in DG and numbers of toxic algal present in the tank. Three profiles of toxin accumulation potential are separated in clusters. Low (blue empty squares), intermediate (yellow empty triangles) and high (red empty circles) accumulation clusters are composed of 5, 8 and 5 scallops, respectively. Three aberrant values were removed from the dataset. Full shapes are means ± SD of all individuals of the corresponding cluster.

Figure 3: Toxin accumulation linked to feeding behavior. a. Individual toxin concentration in scallop digestive gland (DG) at the end of the exposure (day 4, µg STX 100 g^{-1} DG) against the total numbers of *A. minutum* cells consumed for each scallop on days 3&4 per g of scallop (number of cells g^{-1}) for all assays (n=18). The line indicates the adjusted type II regression model. b. Graph shows clearance rates (L h^{-1}) from TC-A assays (days 1&2 exposition to *T. lutea* and *C. muelleri* and days 3&4 exposition to *A. minutum*) measured from day 1 to day 4 and standardized for a 7g scallop in total mass. Data have been highlighted according to the 3 clusters (low, medium and high accumulation potential), each empty shape representing an individual from the low □, medium △ or high ○ accumulation cluster and filled shapes corresponding to the average values for 5h from the low ■, medium ▲ and high ● accumulation clusters.

Figure 4: Toxin accumulation and accumulation potential in great scallop depend on the time of recovery filtration and on clearance rate inhibition. Graphs a&c show individual clearance rate inhibition index (CRII) as a function of respectively final toxin accumulation (µg STX 100 g^{-1} DG) (a) and accumulation potential (c). Graphs b&d show the time for filtration recovery as a function of respectively final toxin accumulation (µg STX 100 g^{-1} DG) (b) and accumulation potential (d). Circles refer to the different accumulation groups: blue for low, yellow for intermediate and red for high accumulation clusters.

Figure 5: No correlation between accumulation potential and toxin accumulation efficiency at days 3&4.

Toxin accumulation efficiency (TAE) corresponding to the ratio of final toxin content in *P. maximus* and the amount of toxin consumed compared to accumulation potential (ratio between final toxin content in DG and numbers of toxic algal present in the tank).

Figure 6: Evolution of standardized respiration rates over the 4 experimental days. a. Graph shows respiration rates (mg O_2 h^{-1}) for a standard 7g scallop in total mass from TC-A assays (days 1&2 exposition to *T. lutea* and *C. muelleri* and days 3&4 exposition to *A. minutum*) measured from day 1 to day 4. Each empty symbol corresponds to all individual measurements performed on the low □, intermediate △ and high ○ accumulation clusters. Filled symbols correspond to the average values for 5h of each accumulation cluster: low ■, intermediate ▲ and high ●. b. Graph shows the daily mean respiration rates (mg O_2 h^{-1}) of all individuals (standard mass of 7g) for each day of experiment (D1-D4). Each bar indicates the mean percent (± SEM) of 18 individuals. Results were considered significantly different for $P<0.01$.

Figure 7: Representative 2-DE gels (pH 4–7, SDS-PAGE 12%) of *Pecten maximus* mantle proteins in TC-NA and TC-A conditions. Successfully identified protein spots are indicated on the 2-DE gels by a line and associated spot number. a. No algae (TC-NA) and b. toxic algae (TC-A) conditions. Details on identified proteins are provided in Table 1. For each condition N=7.

Table 1: MS/MS identified proteins differentially accumulated in *A. minutum* exposed scallops compared to control non-exposed group. List of *Pecten maximus* mantle proteins differentially expressed between the 2 conditions (TC-A/TC-NA) and identified by MS/MS. Values correspond to the Log2 Fold Change (FC) for the normalized volumes of spots between scallops in toxic algae (TC-

A) and in no algae (TC-NA) conditions. Protein abundance changed significantly between the 2 conditions (moderate t-test paired-comparison, fdr < 0.1).

Name	MW	pHi	# peptides	Peptide sequences	FC	Spot #
Major vault protein	96 kDa	5.7	8	SFFLLPGER LLHADQEIR TFKDDFGVVR KEVVIDETIR AIPLDENEGIYVR TAGDEWLFEGPGTYIPR SVQLAIEITTNSQEATAR IPPYYYLHVLDQNLNVTR	-0.6	3
Fructose-bisphosphate aldolase	39 kDa	6.0	10	ATVLCLSR ATEQVLAFTYK KPWPLTFSFGR GILAADESTGSVGKR FAPINVENTEENR IWQGKDENVAAGQK FAPINVENTEENRR ETPSYQAMLENANVLAR VDKGVVPLMGTDNECTTQGLDGLSER TVPPAVAGVTFLSGGQSEEDASINLNAINTDSGR	-0.7	7
Beta-actin	42 kDa	5.3	6	GYSFTTTAER IWHHTFYNELR SYELPDGQVITIGNER VAPEEHPVLLTEAPLNPK DLYANTVLSGGTTMFPGIADR TTGIVLDSGDGVTHTVPIYEGYALPHAILR	1.2	1
Beta-actin	42 kDa		6	GYSFTTTAER IWHHTFYNELR SYELPDGQVITIGNER VAPEEHPVLLTEAPLNPK DLYANTVLSGGTTMFPGIADR TTGIVLDSGDGVTHTVPIYEGYALPHAILR	0.9	12
Beta-actin	42 kDa		6	GYSFTTTAER IWHHTFYNELR SYELPDGQVITIGNER VAPEEHPVLLTEAPLNPK DLYANTVLSGGTTMFPGIADR TTGIVLDSGDGVTHTVPIYEGYALPHAILR	0.5	8
Beta-actin	42 kDa		6	GYSFTTTAER IWHHTFYNELR SYELPDGQVITIGNER VAPEEHPVLLTEAPLNPK DLYANTVLSGGTTMFPGIADR TTGIVLDSGDGVTHTVPIYEGYALPHAILR	0.5	9
Beta-actin	42 kDa		3	GYSFTTTAER SYELPDGQVITIGNER VAPEEHPVLLTEAPLNPK	0.6	10
Paramyosin	99 kDa	5.6	7	LEEAEAFALR VSLQAEVEDLR SQLQVTLDDFKR IRDLEGELEAEQR LSDELRQEQENYK LSEIQIQVNVLVNDKR DLELASAQYEAQESSTR	-1.1	2
Paramyosin	99 kDa		10	LEEAEAFALR VSLQAEVEDLR YEEESEAASILR SQLQVTLDDFKR IRDLEGELEAEQR LSDELRQEQENYK LSEIQIQVNVLVNDKR DLELASAQYEAQESSTR QNLQVQLSALQSDYDNLNAR LTQENFDLQHQVQELDAANAGLAK	-0.9	11
Filamin A	282 kDa	5.5	5	VYVTPSIGDAR YAGSYVAGSPFK FNDEHIPQSPYR GEINQPCEFNIYTR VTYKPTEPGNYVINIK	-0.9	4
Killer cell lectin-like receptor subfamily B member 1B	31 kDa	4.5	6	TEWSTAINR TLSGFENEIR VSTSDIVYTGR LVEFQTNEEAQFVMR TWGSGEPDGGTQTCGCTR NDAYVWVFLSNDEPVDTAVR	0.7	5
Killer cell lectin-like receptor subfamily B member 1B	31 kDa		7	TEWSTAINR TLSGFENEIR VSTSDIVYTGR ILKNEQAELR FEESSLTSEVVR LVEFQTNEEAQFVMR TWGSGEPDGGTQTCGCTR	0.5	6

Figure 1

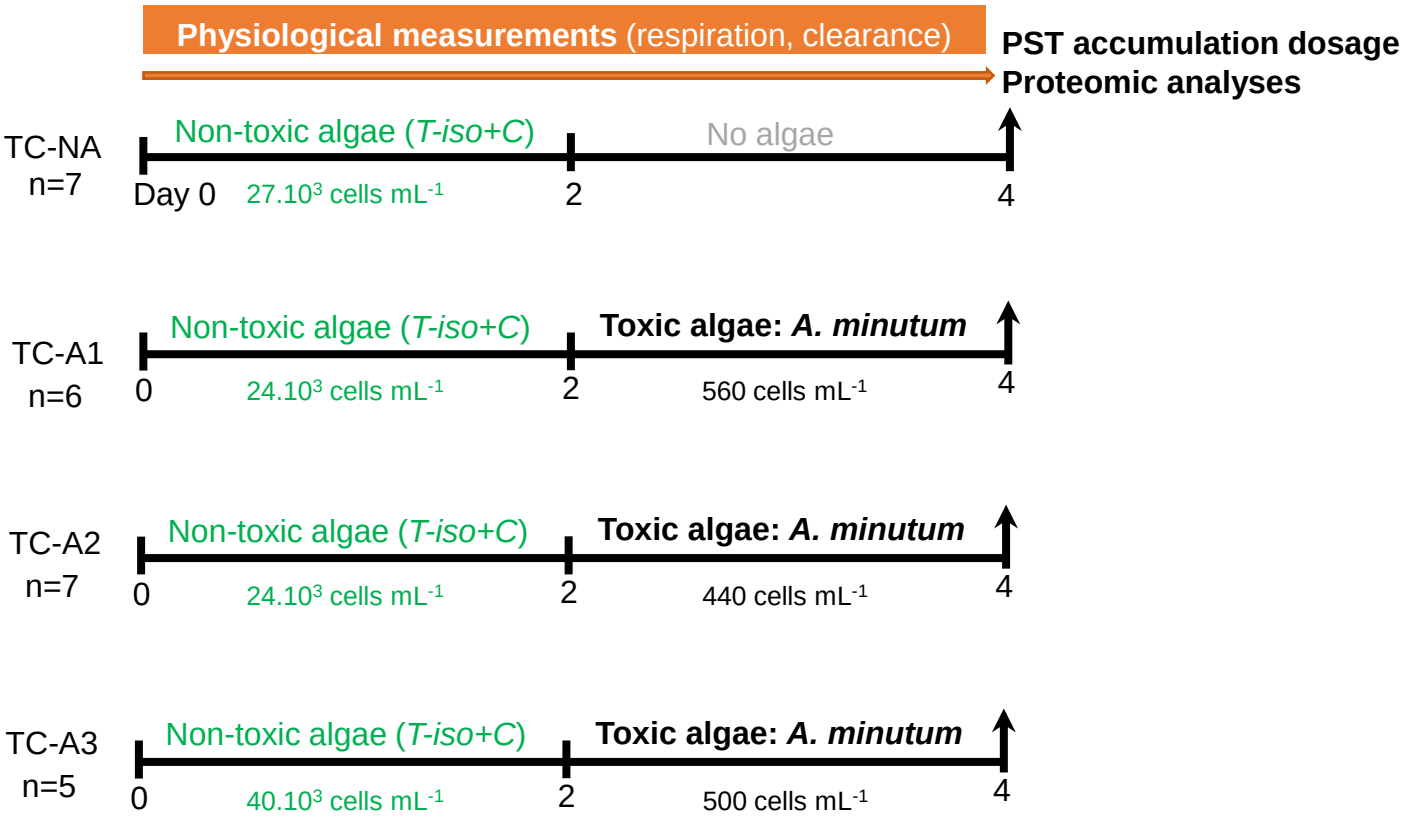
Physiological measurements (respiration, clearance)
PST accumulation dosage
Proteomic analyses
TC-NA
n=7
Non-toxic algae (T-iso+C)
No algae
Day 0
27.10³ cells mL⁻¹
2
4
TC-A1
n=6
Non-toxic algae (T-iso+C)
Toxic algae: A. minutum
0
24.10³ cells mL⁻¹
2
560 cells mL⁻¹
4
TC-A2
n=7
Non-toxic algae (T-iso+C)
Toxic algae: A. minutum
0
24.10³ cells mL⁻¹
2
440 cells mL⁻¹
4
TC-A3
n=5
Non-toxic algae (T-iso+C)
Toxic algae: A. minutum
0
40.10³ cells mL⁻¹
2
500 cells mL⁻¹
4

Figure 2

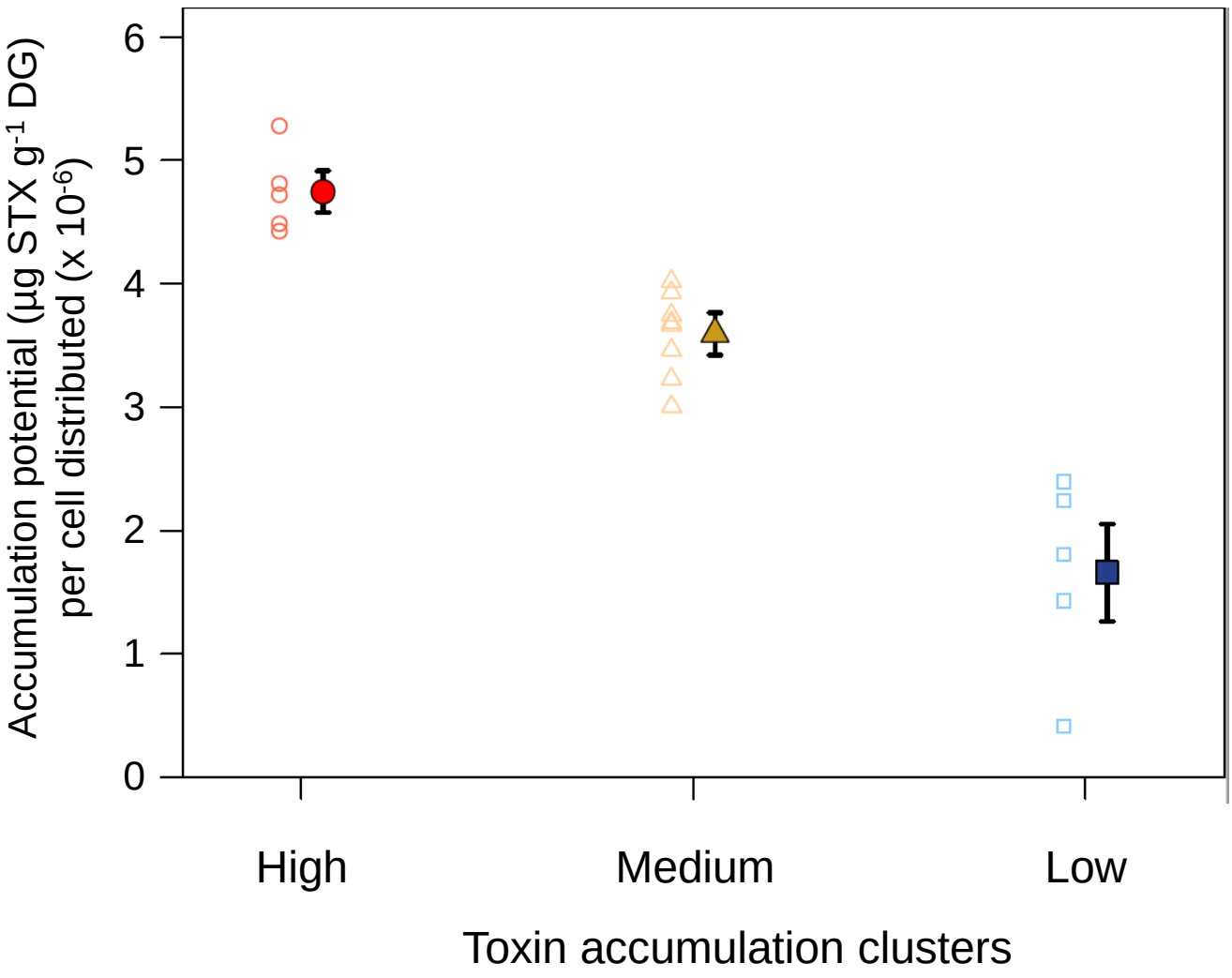
Accumulation potential (µg STX g-1 DG)
per cell distributed (x 10-6)
0
1
2
3
4
5
6
High
Medium
Low
Toxin accumulation clusters

Figure 3

a

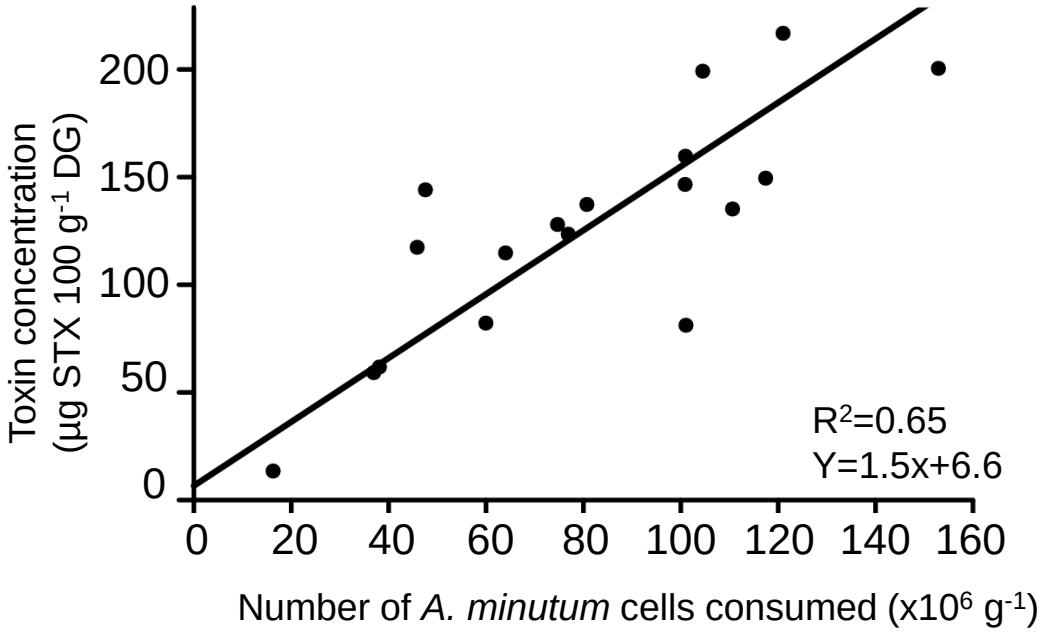
Toxin concentration
(µg STX 100 g-1 DG)
200
150
100
50
0
R2=0.65
Y=1.5x+6.6
0
20
40
60
80
100
120
140
160
Number of A. minutum cells consumed (x106 g-1)

b

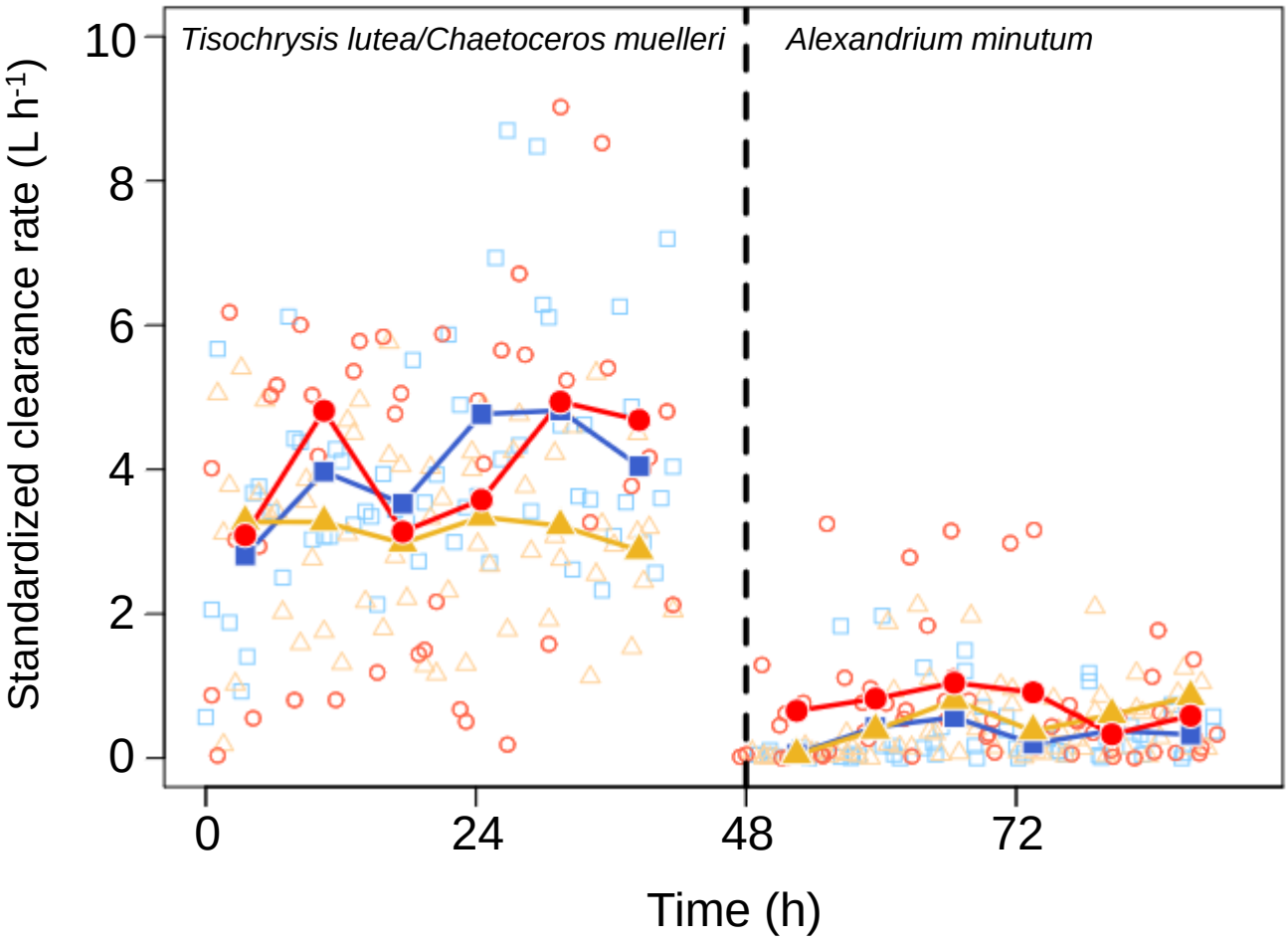
Tisochrysis lutea/Chaetoceros muelleri
Alexandrium minutum
Standardized clearance rate (L h-1)
10
8
6
4
2
0
0
24
48
72
Time (h)

Figure 4

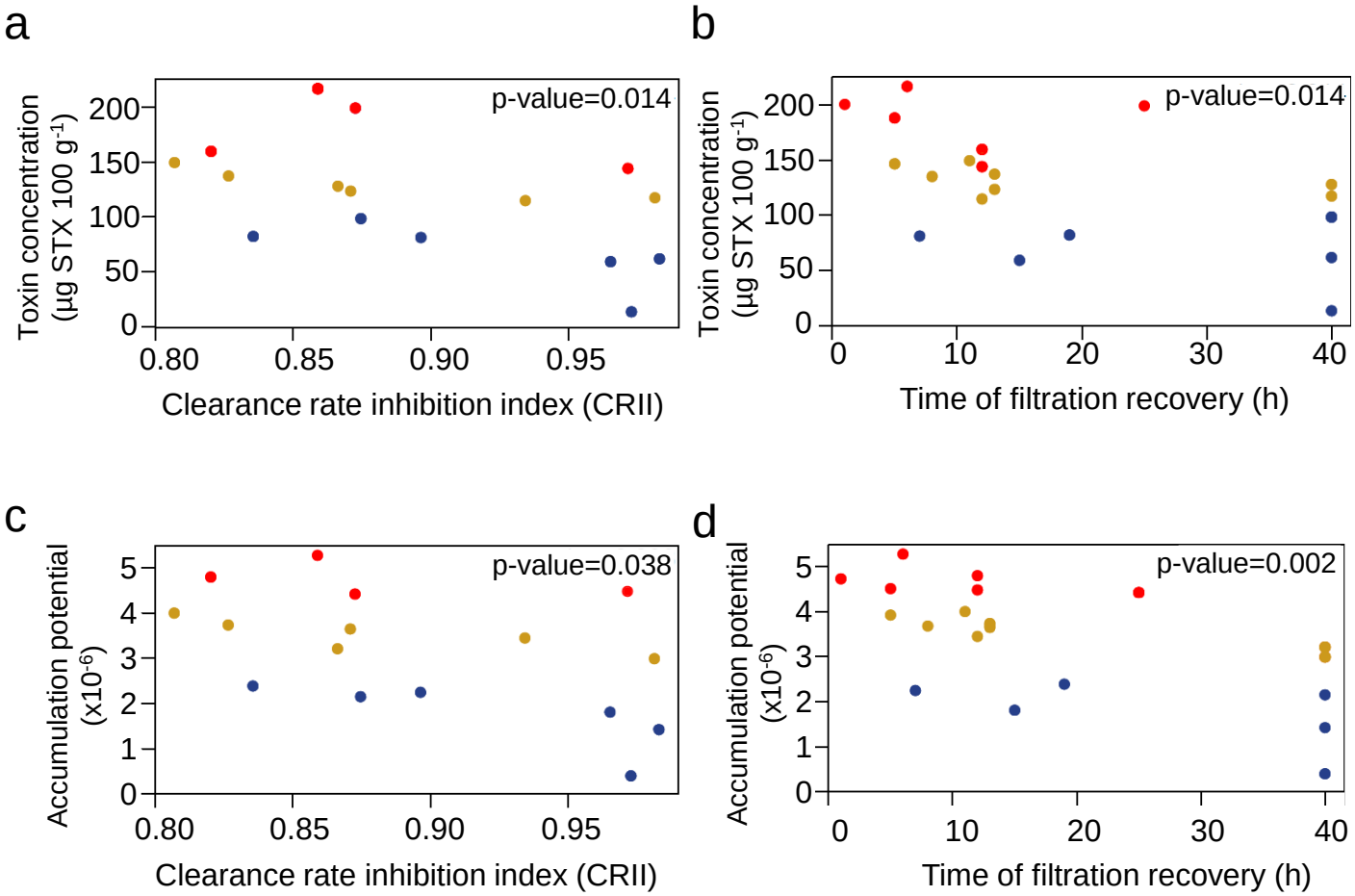
a
b
c
d
p-value=0.014
p-value=0.014
p-value=0.038
p-value=0.002
Toxin concentration (µg STX 100 g-1)
Accumulation potential (x10-6)
Clearance rate inhibition index (CRII)
Time of filtration recovery (h)
0
50
100
150
200
1
2
3
4
5
0.80
0.85
0.90
0.95
10
20
30
40

Figure 5

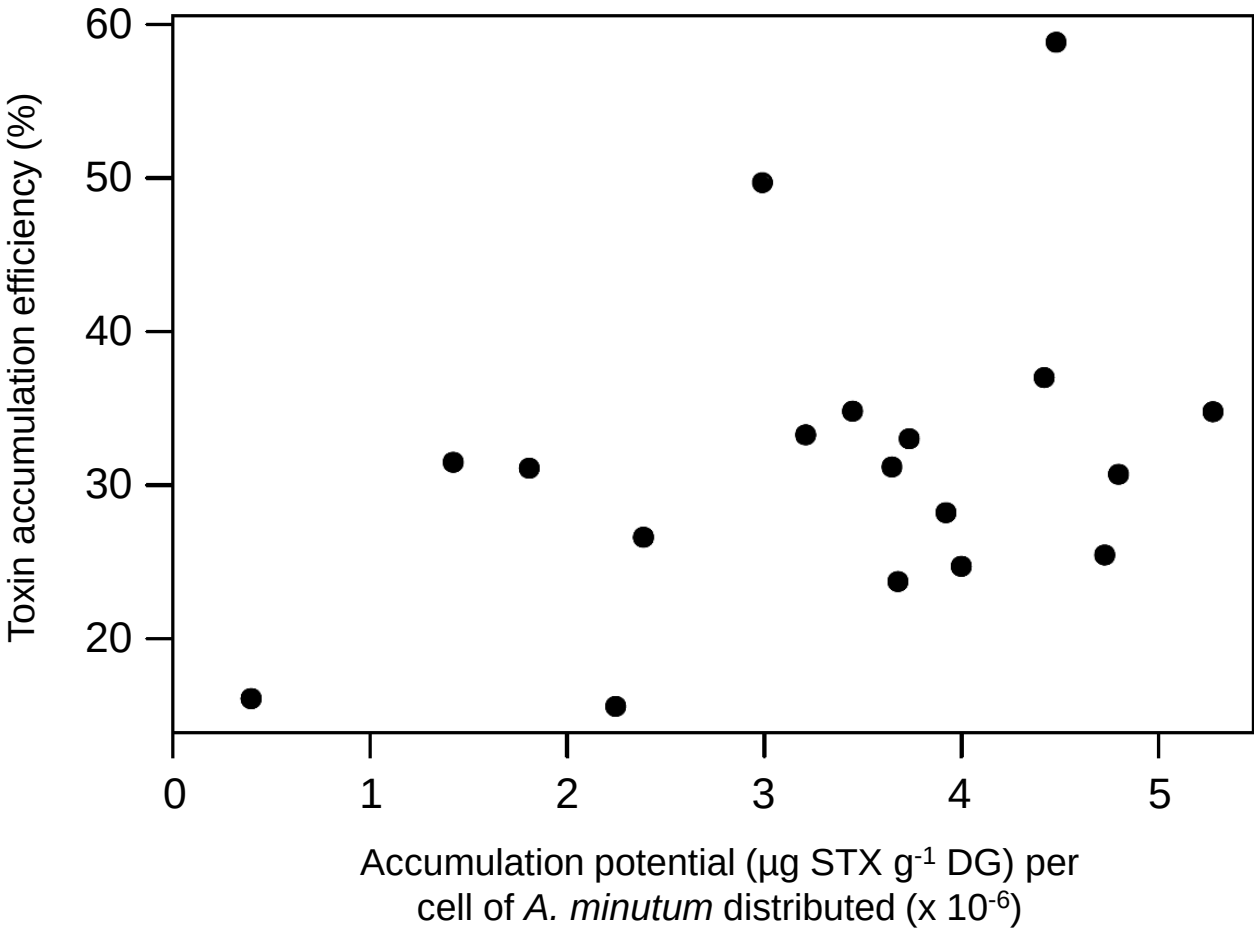
60
50
40
30
20
Toxin accumulation efficiency (%)
0
1
2
3
4
5
Accumulation potential (µg STX g-1 DG) per
cell of A. minutum distributed (x 10-6)

Figure 6

a

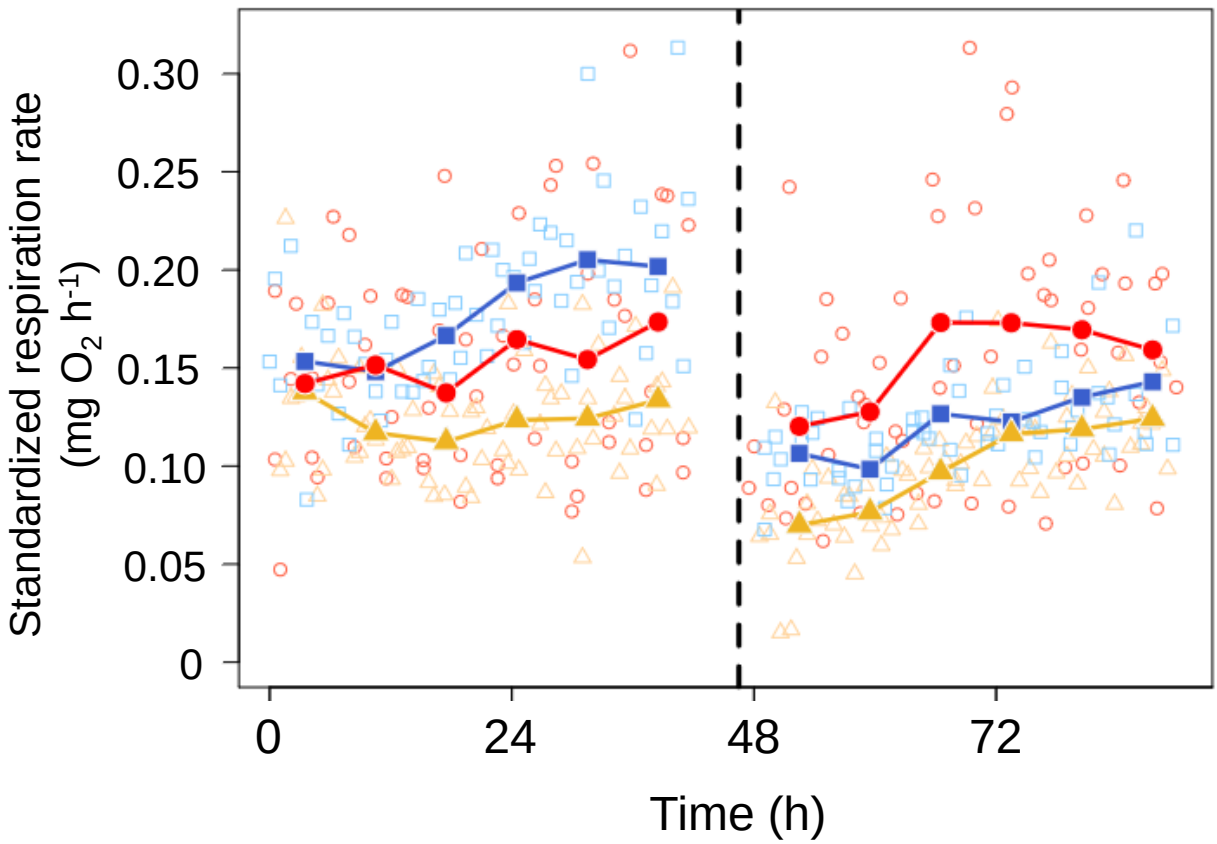
Standardized respiration rate
(mg O2 h-1)
0.30
0.25
0.20
0.15
0.10
0.05
0
0
24
48
72
Time (h)

b

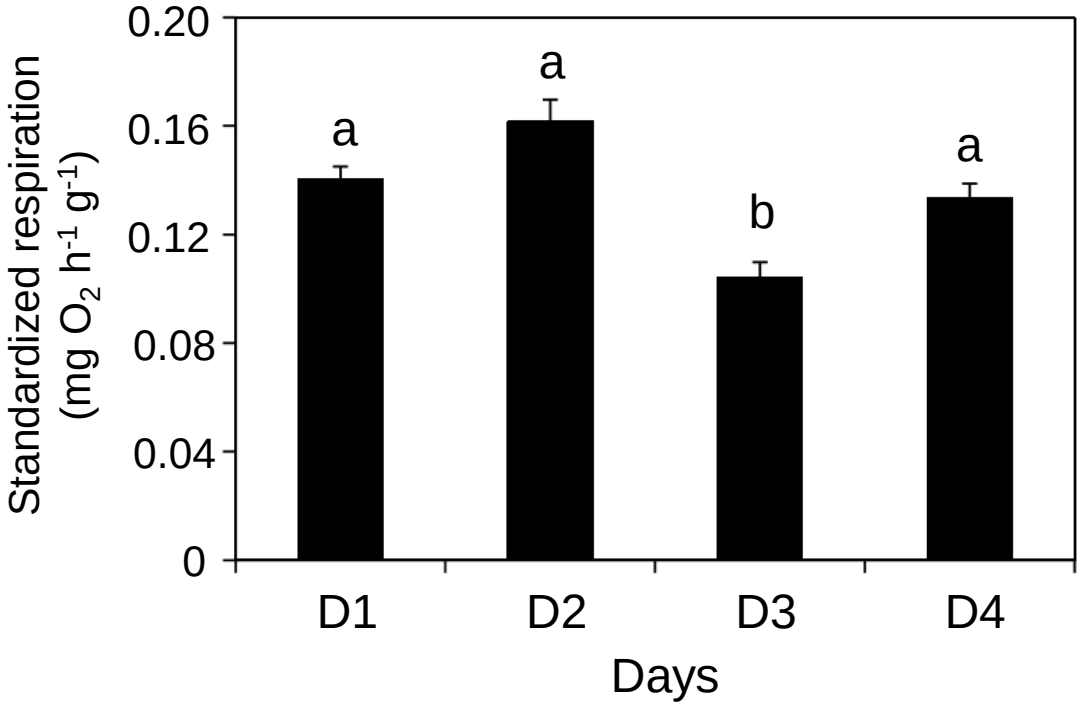
Standardized respiration
(mg O2 h-1 g-1)
0.20
0.16
0.12
0.08
0.04
0
a
a
b
a
D1
D2
D3
D4
Days

Figure 7

a

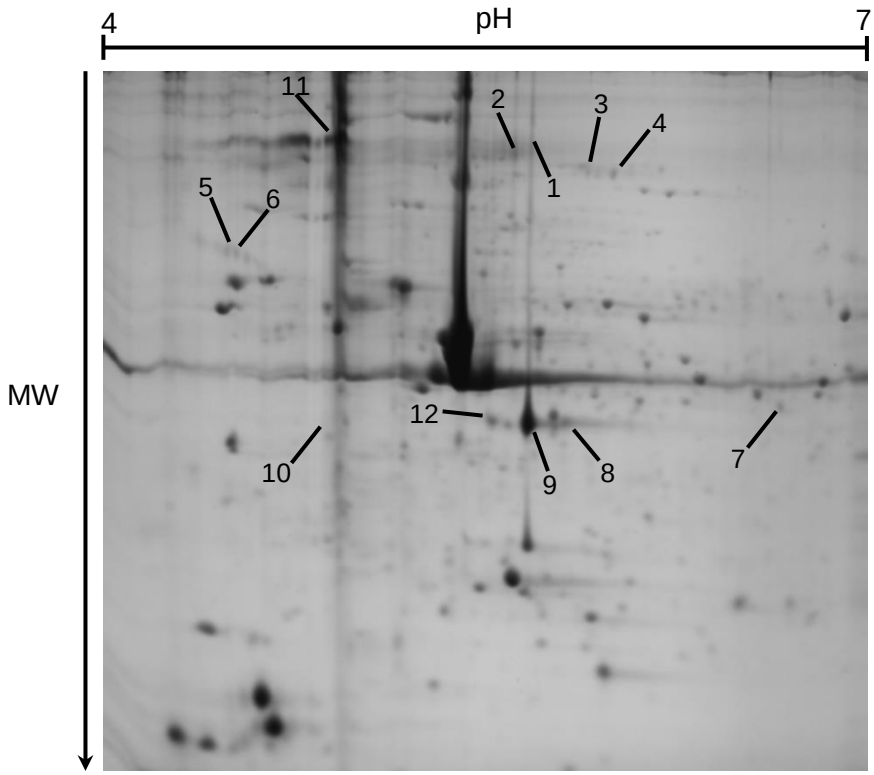

b